

Response functions of cold neutron matter: density, spin and current fluctuations

Jochen Keller and Armen Sedrakian

Institute for Theoretical Physics, J. W. Goethe University, D-60438 Frankfurt am Main, Germany

We study the response of a single-component pair-correlated baryonic Fermi-liquid to density, spin, and their current perturbations. A complete set of response functions is derived in the low-temperature regime both within an effective theory based on a small momentum transfer expansion and within a numerical scheme valid for arbitrary momentum transfers. A comparison of these two approaches validates the perturbative approximation within the domain of its convergence. We derive the spectral functions of collective excitations associated with the density, density-current, spin, and spin-current perturbations. The dispersion relations of density and spin fluctuations are derived and it is shown that the density fluctuations lead to exciton-like undamped bound states, whereas the spin excitations correspond to diffusive modes above the pair-breaking threshold. The contribution of the collective pair-breaking modes to the specific heat of neutron matter at subnuclear densities is computed and is shown to be comparable to that of the degenerate electron gas at not too low temperatures.

PACS numbers: 97.60.Jd, 26.60.+c, 21.65.+f, 13.15.+g

I. INTRODUCTION

The interiors of neutron stars become superfluid shortly after their formation (for reviews of the physics of superfluidity in neutron stars see Refs. [1–5]). In the inner crust of a neutron star the neutrons pair in the 1S_0 channel with the density-dependent gap parameter in the range $\Delta \leq 1$ MeV [3–5]. The neutron S -wave superfluidity persists up to the densities of order of the nuclear saturation density n_0 . Neutron P -wave superfluidity is expected at larger densities [6–8]. Protons, which are less abundant, form an S -wave pair condensate from densities $\sim n_0/2$, where they de-confine from crustal nuclei, up to densities $n \gg n_0$, *i.e.*, the deep interiors of the star. For not too large isospin asymmetries, the D -wave condensation of neutron-proton pairs may set in at high densities as well [9].

The low-energy dynamics of baryonic matter in compact stars can be described, microscopically, in terms of a set of response functions to perturbations having different symmetries. A frequently encountered example is the radiation and transport of neutrinos, in which case one is interested in vector and axial-vector perturbing operators. Response functions also contain the complete information on the spectrum of the low-lying excitations (*i.e.*, density waves, spin waves, etc.) and, therefore, they permit to evaluate the contribution of the collective excitations to thermodynamics and transport of matter.

Near equilibrium the response functions of nuclear systems are characterized by length scales that are large compared to the inverse Fermi wave vector, or equivalently, energies that are small compared to the Fermi energy. In the unpaired limit, the Landau theory of normal Fermi liquids provides a suitable framework for the evaluation of response functions in compact stars [10–16]. The many-body problem of the evaluation of response functions entails a number of challenges. One is the identification of the relevant set of diagrams, when perturbation theory fails. For many systems the response functions are

computed from a resummation of an infinite number of finite temperature ring diagrams [17]. While this scheme accounts for the (vertex renormalized) single particle-hole excitations, it does not include multi-pair contributions to the response functions. Such contributions are important for the evaluation of the magnetic susceptibility of degenerate nuclear matter [10–14]. The second challenge is the inclusion of the non-central forces, which arise in the nuclear systems due to the tensor forces. In fact, these give rise to the coupling of states with more than one quasiparticle-quasihole pair, thereby changing the static susceptibility and the magnetic moments in the nuclear Fermi liquid [10–14]. As a consequence, in nuclear matter the relationship between the Landau parameters and the magnetic susceptibility is considerably more complicated than for systems with purely central forces. Sum-rule arguments can be used to place a lower bound on the contribution to the static susceptibility coming from transitions to multipair states [10, 11]. Furthermore, it was shown that the rates of processes involving transitions to two quasiparticle-quasihole states may be calculated in terms of the collision integral in the Landau transport equation for quasiparticles [12, 13]. The multi-loop processes induced by the tensor forces are of paramount importance in the astrophysics of neutron stars, since the bremsstrahlung processes on weak neutral currents are among the leading processes contributing to the neutrino luminosity of these stars [18–21].

The focus of this paper is the derivation of the response functions associated with perturbations of density, density current, spin, and spin current in a single-component Fermi liquid. It extends our earlier study of density response [22] to new types of perturbations as well as revises some of the perturbative results contained therein. The energy scale characterizing the dynamical processes in neutron stars are of the order of temperature $T \leq 1$ MeV. The high densities in compact stars render the Fermi energies of fermions in the range $\epsilon_F \sim 10 - 100$ MeV. Consequently, one needs the response functions in

the limit $T/\epsilon_F \ll 1$. As mentioned above the pairing gaps could be of the order of 1 MeV, *i.e.*, they substantially influence the dynamics of the systems for temperatures $T \leq T_c$, the critical temperature of the superfluid phase transition.

This study is based on the method of the Green's functions for superfluid systems at non-zero temperatures and aims at the resummation of an infinite series of particle-hole ladder diagrams in neutron matter. This re-summation scheme respects the gauge invariance, sum rules, and baryon number conservation. The appropriate technique was first developed by Abrikosov and Gor'kov in the electrodynamics of superconductors [23] (see also Ref. [24]). In this theory the response of the superconductors to external probes is expressed in the language of propagators at non-zero temperature and density with contact interactions that do not distinguish among the particle-hole and particle-particle channels. It is equivalent to the theories initially advanced by Bogolyubov [25], Anderson [26] and others, which are based on the equations of motion for second-quantized operators. Subsequently, Larkin, Migdal, and Leggett [27, 28] generalized the Landau Fermi-liquid theory to superconductors and superfluids, thus extending the Abrikosov-Gor'kov approach to strongly interacting regime. This last method implements the wave-function renormalization of the quasiparticle spectrum, higher order harmonics in the interaction channels, and postulates particle-hole (ph) and particle-particle (pp) interactions with different strength and/or sign.

The response functions of baryonic matter were studied in the unpaired, but degenerate regime in the context of neutrino emission from compact stars (see, e.g., Ref. [29] and references therein). The work on these functions in the same context, but for superfluid baryonic matter started more recently [30–37].

Quite generally, the response functions to density, spin and their current perturbations can be related to the appropriate response functions of baryons to the operators of the electroweak theory. To see the mapping explicitly consider the weak interaction Lagrangian, which at low energies is given by

$$\mathcal{L}_W = -\frac{G_F}{2\sqrt{2}}(J_V^\mu - J_A^\mu)J_\mu^L, \quad (1)$$

where G_F is the Fermi constant and the vector and axial-vector currents are defined as

$$J_V^\mu = c_V \bar{\Psi}_N \gamma^\mu \Psi_N \simeq c_V \psi_N^\dagger (1, \mathbf{v}_F) \psi_N, \quad (2)$$

$$J_A^\mu = c_A \bar{\Psi}_N \gamma^\mu \gamma_5 \Psi_N \simeq c_A \psi_N^\dagger (\boldsymbol{\sigma} \mathbf{v}_F, \boldsymbol{\sigma}) \psi_N, \quad (3)$$

and $J_\mu^L = \bar{\psi} \gamma_\mu (1 - \gamma_5) \psi$ is the lepton current. Here \mathbf{v}_F is the Fermi velocity of baryons, $\boldsymbol{\sigma}$ is the vector of Pauli-matrices. Here and below the Greek indices run over 0, 1, 2, 3, and label the temporal and three spatial coordinates; the spatial coordinates are also labeled by Latin indices and run through 1, 2, 3. Equations (2) and (3) approximate the baryonic vector and axial-vector weak currents

by their dominant contributions in the non-relativistic limit by keeping the large components of the baryonic Dirac spinors. The bare vertices of interest are thus given by the expression in-between the baryon fields ψ_N^\dagger and ψ_N in Eqs. (2) and (3):

$$\Gamma_0^{D\mu} = (\Gamma_0^D, \mathbf{\Gamma}_0^D) = (1, \mathbf{v}_F), \quad (4)$$

$$\Gamma_0^{S\mu} = (\Gamma_0^S, \mathbf{\Gamma}_0^S) = (\boldsymbol{\sigma} \mathbf{v}_F, \boldsymbol{\sigma}). \quad (5)$$

It is now clear that there is a one-to-one correspondence between weak interaction vertices in the non-relativistic limit and vertices associated with the density and density-current (index D), as well as the spin-current and spin-density perturbations (index S).

One complication that is always present in compact stars is the fact that the matter is multi-component in the crusts and the core of the star. A superfluid features Goldstone bosons associated with the breaking of the baryon $U(1)$ number in a superfluid [38, 39]. Furthermore, the existence of the lattice of nuclei (and non-spherical nuclear phases) in the crust adds the lattice phonons to the set of the collective modes that propagate in the star's crust [40, 41]. The various modes are coupled [39, 42–44]. In the cores of neutron stars there are at least three fluids – the neutron and proton Fermi liquids, which are both expected to be in the superfluid state, and an ultra-relativistic gas of electrons [29]. The density modes associated with the superconducting proton component in the homogeneous matter of the outer core of neutron stars were computed in Refs. [45–47]. It is clear that our treatment of a single-component superfluid nuclear Fermi liquid does not account for coupling among various components. A more complete treatment must take into account the multi-component nature of matter.

This paper is organized as follows. The remainder of the Introduction provides prerequisite information. In Sec. II the baryon propagators and self-energies are introduced within a finite-temperature imaginary-time theory. Vertex functions corresponding to density and spin perturbations are discussed in Sec. III. Section IV is devoted to the density and spin response functions, with two subsections discussing perturbative expansions of response functions as well as their exact numerical evaluation. In Sec. V the spectral functions and collective density and spin excitations are discussed. We evaluate the specific heat contribution arising from these excitations in Sec. VI. Our conclusions are collected in Sec. VII. The details of computations are relegated to Appendices A and B and a comparison to other methods is presented in Appendix C. We use the natural units $\hbar = c = 1$ and assume that the Boltzmann constant $k_B = 1$, with the exception of Sec. VI.

A. Prerequisites

In this study we explore the temperature domain well below the critical temperature of superfluid phase transitions; typically $T/T_c \leq 0.5$, where T_c is the critical temperature of a superfluid transition. This is the case in the dominant majority of observable neutron stars. We further consider densities where the 1S_0 -wave pairing is dominant among neutrons and protons. This assumption confines our study to the densities at and below the nuclear saturation density. In the presumed temperature and density domain it is safe to treat the nucleons as non-relativistic particles, *i.e.*, the Fermi velocity of the particles is small compared to the velocity of light in a vacuum, $v_F \ll 1$ in natural units. This enables us to use the non-relativistic dispersion law for the particles in the normal state and non-relativistic limits of the Dirac matrices appearing in the bare vertices. Furthermore, because we work in the extreme low-temperature limit, we shall restrict the length of the momenta of the particles to their Fermi wave-vector, *i.e.*, we write $\mathbf{p} = m^* v_F \mathbf{n}$, where m^* is the effective mass of a quasiparticle and $\mathbf{n} = \mathbf{p}/|\mathbf{p}|$.

One of the purposes of this work is to compare the response functions obtained from perturbative approaches and direct numerical computation. The perturbative treatment is based on a low-momentum transfer expansion, where the expansion parameter is either generic and reflects the characteristic properties of the system or is dictated by certain kinematical conditions valid in the domain of interest. Examples of small parameters are q/k_F or qv_F/ω , where k_F is the Fermi wave vector, and ω and q are the energy and the magnitude of the momentum transfer. While the first parameter is generic for thermal processes (*i.e.*, processes in which the energy-momentum transfer is of the order of temperature) the second is small only in the kinematical domain of time-like processes (*e.g.*, neutrino radiation). In the second case the momentum transfer is thermal, therefore $q \ll k_F$, which establishes one suitable expansion parameter. We note that for on-shell perturbations with linear spectrum, as, for example, neutrinos ($\omega = q$ in natural units) the smallness of the two expansion parameters reduces to the condition $v_F \ll 1$, which is the same as the non-relativistic expansion. In the case of the numerical computation there are in principle no constraints on the values of the momentum transfer and the Fermi wave vector. However, since our intention is to compare the perturbative and exact numerical results, we will restrict ourselves to the range of values of the parameters defined by the perturbative treatment.

B. Unpaired and pair-correlated particle spectra

As we work in the non-relativistic limit the spectrum in the normal state is given by

$$\xi_p = \frac{p^2}{2m^*} - \mu, \quad (6)$$

where μ is the chemical potential. The spectrum in the pair-correlated case is

$$\epsilon_p = \sqrt{\xi_p^2 + \Delta^2}, \quad (7)$$

where we assume that the gap function is momentum independent, which is the case for contact pairing interactions. We will need frequently the perturbed spectra of particles, which are defined in the unpaired case as

$$\xi_{\pm} = \frac{1}{2m^*} \left(\mathbf{p} \pm \frac{\mathbf{q}^2}{2} \right) - \mu \simeq \xi_p \pm \frac{\mathbf{q}\mathbf{v}}{2}, \quad (8)$$

where in the second expression the small recoil term $\mathbf{q}^2/8m^*$ has been dropped. In the paired case the quasiparticle spectrum is

$$\epsilon_{\pm} = \sqrt{\xi_{\pm}^2 + \Delta^2} \simeq \sqrt{\epsilon_p^2 \pm \xi_p \mathbf{q}\mathbf{v}}, \quad (9)$$

to leading order in $|\mathbf{q}|$.

II. BARYON PROPAGATORS AND SELF-ENERGIES

In a normal Fermi liquid the propagator is defined as

$$\hat{G}_{N,\sigma\sigma'}(\mathbf{p}, \tau - \tau') = -\delta_{\sigma\sigma'} \langle T_{\tau} \psi_{p\sigma}(\tau) \psi_{p\sigma'}^{\dagger}(\tau') \rangle, \quad (10)$$

where τ is the imaginary time, σ is the spin projection, and T_{τ} is the time-ordering operator. The Dyson equation for the normal propagator is given by

$$\hat{G}_N = \hat{G}_0 + \hat{G}_0 \hat{\Sigma} \hat{G}_N, \quad (11)$$

where the index 0 refers to the free-particle propagator and $\hat{\Sigma}$ is the self-energy. A superfluid is described by the following propagators

$$\hat{G}_{\sigma\sigma'}(\mathbf{p}, \tau - \tau') = -\delta_{\sigma\sigma'} \langle T_{\tau} \psi_{p\sigma}(\tau) \psi_{p\sigma'}^{\dagger}(\tau') \rangle, \quad (12)$$

$$\hat{F}_{\sigma\sigma'}(\mathbf{p}, \tau - \tau') = \langle T_{\tau} \psi_{-p\downarrow}(\tau) \psi_{p\uparrow}(\tau') \rangle, \quad (13)$$

$$\hat{F}_{\sigma\sigma'}^+(\mathbf{p}, \tau - \tau') = \langle T_{\tau} \psi_{p\uparrow}^{\dagger}(\tau) \psi_{-p\downarrow}^{\dagger}(\tau') \rangle, \quad (14)$$

$$\hat{G}_{\sigma\sigma'}^-(\mathbf{p}, \tau - \tau') = -\delta_{\sigma\sigma'} \langle T_{\tau} \psi_{-p\sigma}^{\dagger}(\tau) \psi_{-p\sigma'}(\tau') \rangle. \quad (15)$$

These propagators obey Nambu-Gorkov equations and are given by

$$\hat{G} = \hat{G}_0 + \hat{G}_0 \hat{\Sigma} \hat{G} + \hat{G}_0 \hat{\Delta} \hat{F}^+ = \hat{G}_N + \hat{G}_N \hat{\Delta} \hat{F}^+, \quad (16)$$

$$\hat{F}^+ = \hat{G}_0^- \hat{\Sigma}^- \hat{F}^+ + \hat{G}_0^- \hat{\Delta}^+ \hat{G} = \hat{G}_N^- \hat{\Delta}^+ \hat{G}, \quad (17)$$

$$\hat{F} = \hat{G}_0 \hat{\Sigma} \hat{F} + \hat{G}_0 \hat{\Delta} \hat{G}^- = \hat{G}_N \hat{\Delta} \hat{G}^-, \quad (18)$$

$$\hat{G}^- = \hat{G}_0^- + \hat{G}_0^- \hat{\Sigma}^- \hat{G}^- + \hat{G}_0^- \hat{\Delta}^+ \hat{F} = \hat{G}_N^- + \hat{G}_N^- \hat{\Delta}^+ \hat{F}, \quad (19)$$

where $\hat{G}(p)$ and $\hat{G}_0(p)$ are the full and free normal propagators, $\hat{F}(p)$ and $\hat{F}^+(p)$ are the anomalous propagators,

$\hat{\Sigma}(p)$ and $\hat{\Sigma}^-(p)$ are the normal self-energies for particles and holes, and $\hat{\Delta}(p)$ and $\hat{\Delta}^+(p)$ are the anomalous self-energies. The propagators and self-energies are 2×2 -matrices in the spin space. (We suppress the isospin space variables as we consider only single-component ensembles with fixed isospin.) The normal (particle and hole) propagators and self-energies are diagonal in spin space,

$$\hat{G}(p) = G(p)\hat{1}_2 = G^(-p)\hat{1}_2 = \hat{G}^(-p), \quad (20)$$

$$\hat{\Sigma}(p) = \Sigma(p)\hat{1}_2 = \Sigma^(-p)\hat{1}_2 = \hat{\Sigma}^(-p), \quad (21)$$

while the anomalous ones are antisymmetric in spin space and therefore are proportional to $i\sigma_2$,

$$\hat{F}(p) = F(p)i\sigma_2, \quad \hat{F}^+(p) = F^+(p)i\sigma_2 \quad (22)$$

$$\hat{\Delta}(p) = \Delta(p)i\sigma_2, \quad \hat{\Delta}^+(p)i\sigma_2 = \Delta^+(p)i\sigma_2, \quad (23)$$

where σ_2 stands for the second Pauli matrix. For real pairing gaps $\Delta(p) = \Delta^+(p)$ and $F(p) = F^+(p)$.

The propagators can be written as the sum of a pole and a regular part by expanding the self-energy in the vicinity of the Fermi surface. Neglecting the (small) off-shell contributions, we shall keep the pole part of the propagators and set the wave function renormalization $Z(p)^{-1} = 1 - \partial_\omega \Sigma(\omega)|_{\omega=\xi_p} = 1$. The real-time solution of the Nambu-Gorkov equations in momentum space are

$$G = \frac{p_0 + \xi_p}{p_0^2 - \epsilon_p^2 + i\eta} = \frac{u_p^2}{p_0 - \epsilon_p + i\eta} + \frac{v_p^2}{p_0 + \epsilon_p + i\eta}, \quad (24)$$

$$F = \frac{-\Delta}{p_0^2 - \epsilon_p^2 + i\eta} = -u_p v_p \left(\frac{1}{p_0 - \epsilon_p + i\eta} - \frac{1}{p_0 + \epsilon_p + i\eta} \right), \quad (25)$$

with

$$G(p) = G^(-p), \quad (26)$$

$$\Sigma(p) = \Sigma^(-p), \quad (27)$$

$$F(p) = F^+(p) = F(p), \quad (28)$$

$$\Delta(p) = \Delta^+(p) = \Delta, \quad (29)$$

and the Bogolyubov amplitudes defined as

$$u_p = \frac{1}{\sqrt{2}} \left(1 + \frac{\xi_p}{\epsilon_p} \right), \quad (30)$$

$$v_p = \frac{1}{\sqrt{2}} \left(1 - \frac{\xi_p}{\epsilon_p} \right). \quad (31)$$

The finite temperature Matsubara Green's functions are obtained via a replacement of the time-component of the four-momentum in Eqs. (24) and (25) by a complex frequency

$$G(ip_n, \mathbf{p}) = \frac{u_p^2}{ip_n - \epsilon_p} + \frac{v_p^2}{ip_n + \epsilon_p}, \quad (32)$$

$$F(ip_n, \mathbf{p}) = -u_p v_p \left(\frac{1}{ip_n - \epsilon_p} - \frac{1}{ip_n + \epsilon_p} \right), \quad (33)$$

which assumes discrete values $p_n = (2n+1)\pi T$, where n is an integer.

III. VERTEX FUNCTIONS

The equations for vertex functions involve loops which are constructed from the convolutions of a product of two propagators. One possible kinematics for such products is the symmetrical one, which assigns to an arbitrary imaginary-time propagator X the arguments $X_+ = (ip_n + i\omega_m, \mathbf{p} + \frac{\mathbf{q}}{2})$ and $X_- = (ip_n, \mathbf{p} - \frac{\mathbf{q}}{2})$, *i.e.*, the external momentum is split symmetrically among the particle and the hole (but the energy transfer is not). The remainder of this work will use this kinematics. We now turn to the calculation of the effective (or dressed) vertices, which take into account the modifications due to the strong interactions in the medium. The driving interaction in the particle-particle and particle-hole channel will be parametrized as [27]

$$\hat{V}_{\alpha\beta\gamma\delta}^{\text{pp}} \simeq V_{\text{pp}}^D (i\sigma_2)_{\alpha\beta} (i\sigma_2)_{\gamma\delta} + V_{\text{pp}}^S (i\sigma_2 \boldsymbol{\sigma})_{\alpha\beta} \cdot (\boldsymbol{\sigma} i\sigma_2)_{\gamma\delta}, \quad (34)$$

$$\hat{V}_{\alpha\beta\gamma\delta}^{\text{ph}} \simeq V_{\text{ph}}^D \delta_{\alpha\beta} \delta_{\gamma\delta} + V_{\text{ph}}^S \boldsymbol{\sigma}_{\alpha\beta} \cdot \boldsymbol{\sigma}_{\gamma\delta}, \quad (35)$$

where V^D and V^S are the interaction strengths in the density and spin channels, the subscripts or superscripts pp and ph refer to the particle-particle and particle-hole channels, respectively.

Since the particle momenta are restricted to the Fermi surfaces, the amplitudes will depend only on the angle formed by the momenta of the particles. Therefore, as in the ordinary Fermi-liquid theory, they can be expanded in spherical harmonics with respect to this angle. The coefficients in this expansion are the Landau parameters. We will retain the leading-order Landau parameter only, since the higher-order Landau parameters are numerically insignificant. We will use below their values for bulk neutron matter as computed in Ref. [33].

In analogy with the random phase approximation for unpaired ensembles the calculation of full vertices requires a summation of an infinitely long chain of irreducible particle-hole ring diagrams. One possible way to derive these equations is to compute the variations of the Nambu-Gor'kov equations in an external field [27]. Another method to set up the integral equations for the vertices is to construct them directly from Feynman diagrammatic rules. In any case, since a single-component superfluid ensemble is fully described by four different propagators, one finds that there are four topologically different vertices, which are determined by four coupled integral equations. The analytical form of these equations for scalar vertices is

$$\hat{\Gamma}_1^{D/S} - \hat{\Gamma}_0^{D/S} = \int \frac{d^4 p}{(2\pi)^4 i} \hat{V}_{\text{ph}}^{D/S} \left(\hat{G}_1^{D/S} \hat{G} + \hat{F}_3^{D/S} \hat{G} + \hat{G}_2^{D/S} \hat{F} + \hat{F}_4^{D/S} \hat{F} \right), \quad (36)$$

$$\hat{\Gamma}_2^{D/S} = \int \frac{d^4 p}{(2\pi)^{4i}} \hat{V}_{\text{pp}}^{D/S} \left(\hat{G}_2^{D/S} \hat{G}^- + \hat{F} \hat{\Gamma}_4^{D/S} \hat{G}^- + \hat{G}^- \hat{\Gamma}_1^{D/S} \hat{F} + \hat{F} \hat{\Gamma}_3^{D/S} \hat{F} \right), \quad (37)$$

$$\hat{\Gamma}_3^{D/S} = \int \frac{d^4 p}{(2\pi)^{4i}} \hat{V}_{\text{pp}}^{D/S} \left(\hat{G}^- \hat{\Gamma}_3 \hat{G} + \hat{F} \hat{\Gamma}_1^{D/S} \hat{G} + \hat{G}^- \hat{\Gamma}_4^{D/S} \hat{F} + \hat{F} \hat{\Gamma}_2^{D/S} \hat{F} \right), \quad (38)$$

$$\hat{\Gamma}_4^{D/S} - \hat{\Gamma}_0^{D/S-} = \int \frac{d^4 p}{(2\pi)^{4i}} \hat{V}_{\text{ph}}^{D/S} \left(\hat{G}^- \hat{\Gamma}_4^{D/S} \hat{G}^- + \hat{F} \hat{\Gamma}_1^{D/S} \hat{F} + \hat{F} \hat{\Gamma}_2^{D/S} \hat{G}^- + \hat{G}^- \hat{\Gamma}_3^{D/S} \hat{F} \right), \quad (39)$$

where subscripts D and S refer to the density and spin, $\hat{\Gamma}_0^{D/S-}$ is the bare vertex for holes. Identical equations can be written for vector vertices. In the following we approximate the particle-hole and particle-particle interaction amplitudes by the leading-order Landau parameters v_{ph} and v_{pp} . The last of these is determined by the gap equation as follows

$$1 = \nu v_{\text{pp}} \int_0^\Lambda d\xi_p \frac{1 - 2f(\epsilon_p)}{2\epsilon_p}, \quad (40)$$

where $\nu = m^* k_F / 2\pi^2$ is the density of states on the Fermi surface and Λ is the cut-off which regularizes the ultraviolet divergence of the integral.

The solutions of the vertex equations (36) to (39) are described in appendix ???. We find for bare scalar vertex $\Gamma_0^D = 1$

$$\Gamma_1^D(\omega, \mathbf{q}) = \Gamma_4^D(\omega, \mathbf{q}) = \frac{\mathcal{C}(\omega, \mathbf{q})}{\mathcal{C}(\omega, \mathbf{q}) - v_{\text{ph}}^D \mathcal{Q}^+(\omega, \mathbf{q})}, \quad (41)$$

$$\Gamma_3^D(\omega, \mathbf{q}) = -\Gamma_2^D(\omega, \mathbf{q}) = \frac{\mathcal{D}^+(\omega, \mathbf{q})}{\mathcal{C}(\omega, \mathbf{q}) - v_{\text{ph}}^D \mathcal{Q}^+(\omega, \mathbf{q})}, \quad (42)$$

for the bare vector vertex $\Gamma_0^D = \mathbf{v}$

$$\Gamma_{1/4}^D(\omega, \mathbf{q}) = \left[\pm \mathbf{n}_v + \frac{v_{\text{ph}}^D \tilde{\mathcal{Q}}^-(\omega, \mathbf{q})}{\mathcal{C}(\omega, \mathbf{q}) - v_{\text{ph}}^D \mathcal{Q}^+(\omega, \mathbf{q})} \mathbf{n}_q \right] v_F, \quad (43)$$

$$\Gamma_{2/3}^D(\omega, \mathbf{q}) = \pm \left[\tilde{\mathcal{D}}^-(\omega, \mathbf{q}) + \frac{v_{\text{ph}}^D \mathcal{D}^+(\omega, \mathbf{q}) \tilde{\mathcal{Q}}^-(\omega, \mathbf{q})}{\mathcal{C}(\omega, \mathbf{q}) - v_{\text{ph}}^D \mathcal{Q}^+(\omega, \mathbf{q})} \right] \frac{\mathbf{n}_q v_F}{\mathcal{C}(\omega, \mathbf{q})}, \quad (44)$$

for the bare scalar spin-current vertex $\Gamma_0^S = \boldsymbol{\sigma}$

$$\Gamma_{1/4}^S(\omega, \mathbf{q}) = \boldsymbol{\sigma} \left[\mathbf{n}_v \pm \frac{v_{\text{ph}}^S \tilde{\mathcal{Q}}^+(\omega, \mathbf{q}) \mathbf{n}_q}{\mathcal{C}(\omega, \mathbf{q}) - v_{\text{ph}}^S \mathcal{Q}^-(\omega, \mathbf{q})} \right] v_F, \quad (45)$$

$$\Gamma_{2/3}^S(\omega, \mathbf{q}) = \pm \left[\tilde{\mathcal{D}}^+(\omega, \mathbf{q}) \right]$$

$$+ \frac{v_{\text{ph}}^S \mathcal{D}^-(\omega, \mathbf{q}) \tilde{\mathcal{Q}}^+(\omega, \mathbf{q})}{\mathcal{C}(\omega, \mathbf{q}) - v_{\text{ph}}^S \mathcal{Q}^-(\omega, \mathbf{q})} \left] \frac{\boldsymbol{\sigma} \mathbf{n}_q v_F}{\mathcal{C}(\omega, \mathbf{q})}, \quad (46)$$

and, finally, for the bare spin vertex $\Gamma_0^S = \boldsymbol{\sigma}$

$$\Gamma_1^S(\omega, \mathbf{q}) = -\Gamma_4^S(\omega, \mathbf{q}) = \frac{\boldsymbol{\sigma} \mathcal{C}(\omega, \mathbf{q})}{\mathcal{C}(\omega, \mathbf{q}) - v_{\text{ph}}^S \mathcal{Q}^-(\omega, \mathbf{q})}, \quad (47)$$

$$\Gamma_3^S(\omega, \mathbf{q}) = -\Gamma_2^S(\omega, \mathbf{q}) = \frac{\boldsymbol{\sigma} \mathcal{D}^-(\omega, \mathbf{q})}{\mathcal{C}(\omega, \mathbf{q}) - v_{\text{ph}}^S \mathcal{Q}^-(\omega, \mathbf{q})}. \quad (48)$$

The functions on the right-hand side of Eqs. (41) to (48) are defined in Appendix A. The full vertex entering the density response is seen to coincide with the one derived in Refs. [22, 33, 36]. The remainder vertices are in agreement with the ones obtained in Ref. [36].

IV. RESPONSE FUNCTIONS

We start with a general expression for a response function in terms of a current-current correlation function

$$\Pi^{\mu\nu} = \frac{1}{2} \int \frac{d^4 p}{(2\pi)^{4i}} \text{Tr} \left\{ \hat{J}_0^\mu \hat{J}^\nu \right\}, \quad (49)$$

where \hat{J}_0^μ and \hat{J}^ν are the bare and dressed currents. The polarization tensor consists of four different contributions (we drop here the subscripts D/S)

$$\begin{aligned} \Pi^{\mu\nu} &= \frac{1}{2} \int \frac{d^4 p}{(2\pi)^{4i}} \text{Tr} \left[\hat{\Gamma}_0^\mu \hat{G} \left(p + \frac{q}{2} \right) \hat{\Gamma}_1^\nu \hat{G} \left(p - \frac{q}{2} \right) \right] \\ &+ \frac{1}{2} \int \frac{d^4 p}{(2\pi)^{4i}} \text{Tr} \left[\hat{\Gamma}_0^\mu \hat{G} \left(p + \frac{q}{2} \right) \hat{\Gamma}_2^\nu \hat{F} \left(p - \frac{q}{2} \right) \right] \\ &+ \frac{1}{2} \int \frac{d^4 p}{(2\pi)^{4i}} \text{Tr} \left[\hat{\Gamma}_0^\mu \hat{F} \left(p + \frac{q}{2} \right) \hat{\Gamma}_3^\nu \hat{G} \left(p - \frac{q}{2} \right) \right] \\ &+ \frac{1}{2} \int \frac{d^4 p}{(2\pi)^{4i}} \text{Tr} \left[\hat{\Gamma}_0^\mu \hat{F} \left(p + \frac{q}{2} \right) \hat{\Gamma}_4^\nu \hat{F} \left(p - \frac{q}{2} \right) \right]. \end{aligned} \quad (50)$$

The trace should be carried out in the spin space. We can now compute the response functions by substituting the bare and effective vertices corresponding to the desired type of perturbation. For the density response the vertices are $\hat{\Gamma}_{0D}^0$ and $\hat{\Gamma}_{jD}^0$ and we find

$$\Pi_D^{00}(\omega, \mathbf{q}) = \frac{\mathcal{Q}^+(\omega, \mathbf{q})}{\mathcal{C}(\omega, \mathbf{q}) - v_{\text{ph}}^D \mathcal{Q}^+(\omega, \mathbf{q})}. \quad (51)$$

Furthermore, the density-current response is given by (summation over repeated indices is assumed)

$$\begin{aligned} \Pi_D^{jj}(\omega, \mathbf{q}) &= \left\{ \mathcal{A}^-(\omega, \mathbf{q}) - \frac{\tilde{\mathcal{B}}(\omega, \mathbf{q}) \tilde{\mathcal{D}}^-(\omega, \mathbf{q})}{\mathcal{C}(\omega, \mathbf{q})} \right. \\ &\left. + \frac{v_{\text{ph}}^D \tilde{\mathcal{Q}}^+(\omega, \mathbf{q}) \tilde{\mathcal{Q}}^-(\omega, \mathbf{q})}{\mathcal{C}(\omega, \mathbf{q})^2 - v_{\text{ph}}^D \mathcal{C}(\omega, \mathbf{q}) \mathcal{Q}^+(\omega, \mathbf{q})} \right\} v_F^2, \end{aligned} \quad (52)$$

the spin-current response is given by

$$\begin{aligned} \Pi_S^{00}(\omega, \mathbf{q}) &= \left\{ \mathcal{A}^+(\omega, \mathbf{q}) - \frac{\tilde{\mathcal{B}}(\omega, \mathbf{q})\tilde{\mathcal{D}}^+(\omega, \mathbf{q})}{\mathcal{C}(\omega, \mathbf{q})} \right. \\ &\quad \left. + \frac{v_{\text{ph}}^S \tilde{\mathcal{Q}}^-(\omega, \mathbf{q})\tilde{\mathcal{Q}}^+(\omega, \mathbf{q})}{\mathcal{C}(\omega, \mathbf{q})^2 - v_{\text{ph}}^S \mathcal{C}(\omega, \mathbf{q})\mathcal{Q}^-(\omega, \mathbf{q})} \right\} v_F^2, \end{aligned} \quad (53)$$

and finally, the spin-density response is

$$\Pi_S^{jj}(\omega, \mathbf{q}) = \frac{3\mathcal{Q}^-(\omega, \mathbf{q})}{\mathcal{C}(\omega, \mathbf{q}) - v_{\text{ph}}^S \mathcal{Q}^-(\omega, \mathbf{q})}. \quad (54)$$

The functions appearing on the right-hand side of Eqs. (52) to (54) are defined in Appendix A. For density perturbations the off-diagonal elements of the polarization tensor with mixed temporal and spatial indices are given by (below for the sake of brevity we drop the arguments of the loops)

$$\Pi_D^{i0}(\omega, \mathbf{q}) = \int \frac{d\Omega}{4\pi} \left\{ \frac{A^+ \mathcal{C} - B\mathcal{D}^+}{\mathcal{C} - v_{\text{ph}}^S \mathcal{Q}^+} \right\} \mathbf{n}_v^i v_F, \quad (55)$$

and

$$\begin{aligned} \Pi_D^{0j}(\omega, \mathbf{q}) &= \int \frac{d\Omega}{4\pi} \left\{ A^- \mathbf{n}_v^j - B \left(\frac{\tilde{\mathcal{D}}^-}{\mathcal{C}} \right) \mathbf{n}_q^j \right. \\ &\quad \left. + \frac{v_{\text{ph}}^D (A^+ \mathcal{C} - B\mathcal{D}^+) \tilde{\mathcal{Q}}^-}{\mathcal{C}^2 - v_{\text{ph}}^D \mathcal{C} \mathcal{Q}^+} \mathbf{n}_q^j \right\} v_F, \end{aligned} \quad (56)$$

while for spin-perturbations they are given by

$$\begin{aligned} \Pi_S^{i0}(\omega, \mathbf{q}) &= \int \frac{d\Omega}{4\pi} \left\{ A^+ \mathbf{n}_v^i - B \left(\frac{\tilde{\mathcal{D}}^+}{\mathcal{C}} \right) \mathbf{n}_q^i \right. \\ &\quad \left. + \frac{v_{\text{ph}}^S (A^- \mathcal{C} - B\mathcal{D}^-) \tilde{\mathcal{Q}}^+}{\mathcal{C}^2 - v_{\text{ph}}^S \mathcal{C} \mathcal{Q}^-} \mathbf{n}_q^i \right\} v_F, \end{aligned} \quad (57)$$

$$\Pi_S^{0j}(\omega, \mathbf{q}) = \int \frac{d\Omega}{4\pi} \left\{ \frac{A^- \mathcal{C} - B\mathcal{D}^-}{\mathcal{C} - v_{\text{ph}}^S \mathcal{Q}^-} \right\} \mathbf{n}_v^j v_F. \quad (58)$$

Each of the polarization tensors can be decomposed into transverse and longitudinal parts with respect to the direction of the momentum transfer \mathbf{q} according to

$$\Pi_L(\omega, \mathbf{q}) = \Pi^{00}(\omega, \mathbf{q}), \quad (59)$$

$$\Pi_T(\omega, \mathbf{q}) = \frac{1}{2} (\delta^{ij} - \mathbf{n}_q^i \mathbf{n}_q^j) \Pi^{ij}(\omega, \mathbf{q}). \quad (60)$$

Performing the decomposition of the vector polarization tensor we obtain for the longitudinal projection

$$\Pi_{V,L}(\omega, \mathbf{q}) = \frac{\mathcal{Q}^+(\omega, \mathbf{q})}{\mathcal{C}(\omega, \mathbf{q}) - v_{\text{ph}}^D \mathcal{Q}^+(\omega, \mathbf{q})} \quad (61)$$

and for transverse projection

$$\Pi_{V,T}(\omega, \mathbf{q}) = \frac{v_F^2}{2} \int \frac{d\Omega}{4\pi} \left\{ A^-(\omega, \mathbf{q}) - A^-(\omega, \mathbf{q}) (\mathbf{n}_v^j \mathbf{n}_q^j)^2 \right\}. \quad (62)$$

The longitudinal and transverse components of the axial-vector polarization read

$$\begin{aligned} \Pi_{A,L}(\omega, \mathbf{q}) &= \left\{ \mathcal{A}^+(\omega, \mathbf{q}) - \frac{\tilde{\mathcal{B}}(\omega, \mathbf{q})\tilde{\mathcal{D}}^+(\omega, \mathbf{q})}{\mathcal{C}(\omega, \mathbf{q})} \right. \\ &\quad \left. + \frac{v_{\text{ph}}^S \tilde{\mathcal{Q}}^-(\omega, \mathbf{q})\tilde{\mathcal{Q}}^+(\omega, \mathbf{q})}{\mathcal{C}(\omega, \mathbf{q})^2 - v_{\text{ph}}^S \mathcal{C}(\omega, \mathbf{q})\mathcal{Q}^-(\omega, \mathbf{q})} \right\} v_F^2, \end{aligned} \quad (63)$$

$$\Pi_{A,T}(\omega, \mathbf{q}) = \frac{\mathcal{Q}^-(\omega, \mathbf{q})}{\mathcal{C}(\omega, \mathbf{q}) - v_{\text{ph}}^S \mathcal{Q}^-(\omega, \mathbf{q})}. \quad (64)$$

These results, which are valid for arbitrary orientations of the external vectors fields, can be further simplified by a suitable choice of the coordinate system.

A. Perturbative results

We now expand the loop functions with respect to the small parameter $y = q/k_F$ and keep contributions up to fourth order in this parameter. The thermal function \mathcal{G} depends on y and $x \equiv \mathbf{n}_q \cdot \mathbf{n}_v$, therefore, we can write

$$\mathcal{G} = \sum_{k=0}^{\infty} \mathcal{G}_{2k} x^{2k} y^{2k} = \mathcal{G}_0 + \mathcal{G}_2 x^2 y^2 + \mathcal{G}_4 x^4 y^4 + \mathcal{O}(y^6). \quad (65)$$

The expansions of the loop functions contain only even functions of the parameter y , since possible odd terms will disappear after angle integration; thus, *e.g.*, for the \mathcal{A} -loop we obtain

$$\mathcal{A} = \mathcal{A}_0 + \mathcal{A}_2 y^2 + \mathcal{A}_4 y^4 + \mathcal{O}(y^6), \quad (66)$$

and similarly for the other three. In practice, we expand the pre-factors in Eqs. (A25) to (A28) as well as the function \mathcal{G} in the power series in parameter y and subsequently combine them. This leads us to the following explicit expressions:

$$\begin{aligned} \nu^{-1} \mathcal{A}^+ &= - \int \frac{d\Omega}{4\pi} \left[1 + \frac{4\mu^2 x^2}{\omega^2} y^2 + \frac{16\mu^4 x^4}{\omega^4} y^4 \right] \mathcal{G}(\mathbf{v}, \mathbf{q}, \mathbf{v}, \mathbf{q}) \\ &\quad - \left[\mathcal{G}_0 + \left(\frac{4\mu^2}{3\omega^2} \mathcal{G}_0 + \frac{1}{3} \mathcal{G}_2 \right) y^2 \right. \\ &\quad \left. + \left(\frac{16\mu^4}{5\omega^4} \mathcal{G}_0 + \frac{4\mu^2}{5\omega^2} \mathcal{G}_2 + \frac{1}{5} \mathcal{G}_4 \right) y^4 \right], \end{aligned} \quad (67)$$

$$\begin{aligned} \nu^{-1} \mathcal{A}^- &= - \int \frac{d\Omega}{4\pi} \left[\frac{4\mu^2 x^2}{\omega^2} y^2 + \frac{16\mu^4 x^4}{\omega^4} y^4 \right] \mathcal{G}(\mathbf{v}, \mathbf{q}, \mathbf{v}, \mathbf{q}) \\ &\quad - \left[\frac{4\mu^2}{3\omega^2} \mathcal{G}_0 y^2 + \left(\frac{16\mu^4}{5\omega^4} \mathcal{G}_0 + \frac{4\mu^2}{5\omega^2} \mathcal{G}_2 \right) y^4 \right], \end{aligned} \quad (68)$$

where we have dropped terms $\mathcal{O}(y^5)$ and higher. Note that the term $\mathcal{G}(\mathbf{q}, \mathbf{v}, \mathbf{qv})$ is purely real, *i.e.*, does not contribute to the imaginary parts of the loops. For fixed momentum transfer it is constant and yields numerically negligible contribution. For the remaining loops we obtain

$$\nu^{-1}\mathcal{B} = -\frac{\omega}{2\Delta}\mathcal{G}_0 - \frac{\omega}{6\Delta}\mathcal{G}_2 y^2 - \frac{\omega}{10\Delta}\mathcal{G}_4 y^4, \quad (69)$$

$$\begin{aligned} \nu^{-1}\mathcal{C} &= \frac{\omega^2}{4\Delta^2}\mathcal{G}_0 + \left(-\frac{\mu^2}{3\Delta^2}\mathcal{G}_0 + \frac{\omega^2}{12\Delta^2}\mathcal{G}_2\right)y^2 \\ &+ \left(-\frac{\mu^2}{5\Delta^2}\mathcal{G}_2 + \frac{\omega^2}{20\Delta^2}\mathcal{G}_4\right)y^4, \end{aligned} \quad (70)$$

$$\nu^{-1}\mathcal{D}^+ = \frac{\omega}{2\Delta}\mathcal{G}_0 + \frac{\omega}{6\Delta}\mathcal{G}_2 y^2 + \frac{\omega}{10\Delta}\mathcal{G}_4 y^4, \quad (71)$$

$$\nu^{-1}\mathcal{D}^- = \int \frac{d\Omega}{4\pi} \left[\frac{\mu x}{\Delta}\mathcal{G}_0 y + \frac{\mu x^3}{\Delta}\mathcal{G}_3 y^3 \right] = 0. \quad (72)$$

One can now readily identify the coefficients of the expansion (66) and its counterparts for the remaining loops. In full analogy, an expansion of the polarization tensors is given as

$$\Pi_{D/S}^{\mu\nu} = \Pi_{D/S,0}^{\mu\nu} + \Pi_{D/S,2}^{\mu\nu} y^2 + \Pi_{D/S,4}^{\mu\nu} y^4 + \mathcal{O}(y^6). \quad (73)$$

The coefficients of the density response function are

$$\Pi_{D0}^{00} = \frac{\mathcal{Q}_0}{\mathcal{C}_0 - v_{\text{ph}}^D \mathcal{Q}_0}, \quad (74)$$

$$\begin{aligned} \Pi_{D2}^{00} &= \frac{\mathcal{A}_2^+ \mathcal{C}_0^2 - \mathcal{B}_2 \mathcal{C}_0 \mathcal{D}_0^+ + \mathcal{B}_0 \mathcal{C}_2 \mathcal{D}_0^+ - \mathcal{B}_0 \mathcal{C}_0 \mathcal{D}_2^+}{\left[\mathcal{C}_0 - v_{\text{ph}}^D \mathcal{Q}_0\right]^2}, \\ & \quad (75) \end{aligned}$$

$$\begin{aligned} \Pi_{D4}^{00} &= \frac{\mathcal{A}_4^+ \mathcal{C}_0 + \mathcal{A}_2^+ \mathcal{C}_2 + \mathcal{A}_0^+ \mathcal{C}_4}{\mathcal{C}_0 - v_{\text{ph}}^D \mathcal{Q}_0} \\ &- \frac{\mathcal{B}_4 \mathcal{D}_0^+ + \mathcal{B}_2 \mathcal{D}_2^+ + \mathcal{B}_0 \mathcal{D}_4^+}{\mathcal{C}_0 - v_{\text{ph}}^D \mathcal{Q}_0} \\ &- \frac{(\mathcal{A}_2^+ \mathcal{C}_0 + \mathcal{A}_0^+ \mathcal{C}_2 - \mathcal{B}_2 \mathcal{D}_0^+ - \mathcal{B}_0 \mathcal{D}_2^+) \mathcal{C}_2}{\left[\mathcal{C}_0 - v_{\text{ph}}^D \mathcal{Q}_0\right]^2} \\ &+ \frac{(\mathcal{A}_0^+ \mathcal{C}_0 - \mathcal{B}_0 \mathcal{D}_0^+) \mathcal{C}_2^2}{\left[\mathcal{C}_0 - v_{\text{ph}}^D \mathcal{Q}_0\right]^3} \\ &- \frac{(\mathcal{A}_0^+ \mathcal{C}_0 - \mathcal{B}_0 \mathcal{D}_0^+) \mathcal{C}_4}{\left[\mathcal{C}_0 - v_{\text{ph}}^D \mathcal{Q}_0\right]^2}, \end{aligned} \quad (76)$$

where

$$\mathcal{Q}_0 = \mathcal{A}_0^+ \mathcal{C}_0 - \mathcal{B}_0 \mathcal{D}_0^+, \quad (77)$$

$$\mathcal{C}_2 = \mathcal{C}_2 - v_{\text{ph}} (\mathcal{A}_2^+ \mathcal{C}_0 + \mathcal{A}_0^+ \mathcal{C}_2 - \mathcal{B}_2 \mathcal{D}_0^+ - \mathcal{B}_0 \mathcal{D}_2^+), \quad (78)$$

$$\begin{aligned} \mathcal{C}_4 &= \mathcal{C}_4 - v_{\text{ph}} (\mathcal{A}_4^+ \mathcal{C}_0 + \mathcal{A}_2^+ \mathcal{C}_2 + \mathcal{A}_0^+ \mathcal{C}_4 \\ &- \mathcal{B}_4 \mathcal{D}_0^+ - \mathcal{B}_2 \mathcal{D}_2^+ - \mathcal{B}_0 \mathcal{D}_4^+). \end{aligned} \quad (79)$$

However, it turns out that $\mathcal{Q}_0 = 0$ and

$$\mathcal{A}_2^+ \mathcal{C}_0^2 - \mathcal{B}_2 \mathcal{C}_0 \mathcal{D}_0^+ + \mathcal{B}_0 \mathcal{C}_2 \mathcal{D}_0^+ - \mathcal{B}_0 \mathcal{C}_0 \mathcal{D}_2^+ = 0. \quad (80)$$

Consequently, the expansion coefficients of the polarization tensor are

$$\Pi_{D0}^{00} = 0, \quad (81)$$

$$\Pi_{D2}^{00} = 0, \quad (82)$$

$$\begin{aligned} \Pi_{D4}^{00} &= \frac{1}{\mathcal{C}_0} \left(\mathcal{A}_4^+ \mathcal{C}_0 + \mathcal{A}_2^+ \mathcal{C}_2 + \mathcal{A}_0^+ \mathcal{C}_4 \right. \\ &\quad \left. - \mathcal{B}_4 \mathcal{D}_0^+ - \mathcal{B}_2 \mathcal{D}_2^+ - \mathcal{B}_0 \mathcal{D}_4^+ \right), \end{aligned} \quad (83)$$

i.e., the density response function obtains a non-zero contribution at order y^4 . The coefficients for the current response are

$$\Pi_{D0}^{jj} = 0, \quad (84)$$

$$\Pi_{D2}^{jj} = \left\{ \mathcal{A}_2^- - \frac{\tilde{\mathcal{B}}_1 \tilde{\mathcal{D}}_1^-}{\mathcal{C}_0} + \frac{v_{\text{ph}}^D \tilde{\mathcal{A}}_1^- \mathcal{C}_0 (\tilde{\mathcal{A}}_1^+ \mathcal{C}_0 - \tilde{\mathcal{B}}_1 \mathcal{D}_0^+)}{\mathcal{C}_0} \right\} v_F^2, \quad (85)$$

$$\begin{aligned} \Pi_{D4}^{jj} &= \left\{ \mathcal{A}_4^- - \frac{\tilde{\mathcal{B}}_1 \mathcal{C}_0 \tilde{\mathcal{D}}_3^- - \tilde{\mathcal{B}}_1 \mathcal{C}_2 \tilde{\mathcal{D}}_1^- + \tilde{\mathcal{B}}_3 \mathcal{C}_0 \tilde{\mathcal{D}}_1^-}{\mathcal{C}_0^2} \right. \\ &+ v_{\text{ph}}^D \left[\frac{(\tilde{\mathcal{A}}_3^- \mathcal{C}_0^2 + 2\tilde{\mathcal{A}}_1^- \mathcal{C}_0 \mathcal{C}_2 - \tilde{\mathcal{A}}_1^- \mathcal{C}) (\tilde{\mathcal{A}}_1^+ \mathcal{C}_0 - \tilde{\mathcal{B}}_1 \mathcal{D}_0^+)}{\mathcal{C}_0^2} \right. \\ &\quad \left. \left. + \tilde{\mathcal{A}}_1^- (\tilde{\mathcal{A}}_1^+ \mathcal{C}_2 + \tilde{\mathcal{A}}_3^+ \mathcal{C}_0 - \tilde{\mathcal{B}}_1 \mathcal{D}_2^+ - \tilde{\mathcal{B}}_3 \mathcal{D}_0^+) \right] \right\} v_F^2, \end{aligned} \quad (86)$$

where

$$\begin{aligned} \mathcal{C} &= 2\mathcal{C}_0 \mathcal{C}_2 - v_{\text{ph}}^D (\mathcal{A}_2^+ \mathcal{C}_0^2 + \mathcal{A}_0^+ \mathcal{C}_0 \mathcal{C}_2 - \mathcal{B}_0 \mathcal{C}_0 \mathcal{D}_2^+ \\ &- \mathcal{B}_0 \mathcal{C}_2 \mathcal{D}_0^+ - \mathcal{B}_2 \mathcal{C}_0 \mathcal{D}_0^+). \end{aligned} \quad (87)$$

In the case of the current response the first non-zero term arises at the order y^2 and the fourth order term is sub-leading.

Note that the vector current polarization tensor must vanish at the zeroth order as required by the f -sum rule [17]

$$\lim_{\mathbf{q} \rightarrow 0} \int d\omega \omega \text{Im} \Pi^D(\mathbf{q}, \omega) = 0. \quad (88)$$

This is a direct consequence of the conservation of the baryon number. For the spin-current response we find

$$\Pi_{S0}^{00} = \mathcal{A}_0^+ v_F^2, \quad (89)$$

$$\Pi_{S2}^{00} = \left\{ \mathcal{A}_2^+ + v_{\text{ph}}^S (\tilde{\mathcal{A}}_1^+ \tilde{\mathcal{A}}_1^- \mathcal{C}_0 \tilde{\mathcal{A}}_1^+ \tilde{\mathcal{A}}_1^- \mathcal{C}_0) \right\} v_F^2, \quad (90)$$

$$\Pi_{S4}^{00} = \left\{ \mathcal{A}_4^+ + v_{\text{ph}}^S (\tilde{\mathcal{A}}_3^+ \tilde{\mathcal{A}}_1^- \mathcal{C}_0 + \tilde{\mathcal{A}}_1^+ \tilde{\mathcal{A}}_3^- \mathcal{C}_0 + \tilde{\mathcal{A}}_1^+ \tilde{\mathcal{A}}_1^- \mathcal{C}_2 \right.$$

$$\begin{aligned}
& -\tilde{\mathcal{A}}_3^- \tilde{\mathcal{B}}_1 \mathcal{D}_0^+ - \tilde{\mathcal{A}}_1^- \tilde{\mathcal{B}}_3 \mathcal{D}_0^+ - \tilde{\mathcal{A}}_1^- \tilde{\mathcal{B}}_1 \mathcal{D}_2^+ \\
& + (v_{\text{ph}}^S)^2 \left(\tilde{\mathcal{A}}_1^+ \tilde{\mathcal{A}}_1^- \mathcal{A}_2^- \mathcal{C}_0 + \tilde{\mathcal{A}}_1^+ \tilde{\mathcal{B}}_1 \mathcal{A}_2^- \mathcal{C}_0 \right) \} v_F^2.
\end{aligned} \tag{91}$$

In this case the leading order contribution, given by Eq. (89), is of order y^0 in the y -expansion, which means that the vertex corrections introduce sub-leading order corrections and the single-loop result is a good approximation to the full polarization tensor. Finally, the spin-density response is given by

$$\Pi_{S0}^{jj} = 0, \tag{92}$$

$$\Pi_{S2}^{jj} = 3 \mathcal{A}_2^- v_F^2, \tag{93}$$

$$\Pi_{S4}^{jj} = 3 (\mathcal{A}_4^- + v_{\text{ph}}^S \mathcal{A}_2^{-2}) v_F^2. \tag{94}$$

The leading order contribution now arises at order y^2 .

If we restrict ourselves only to the leading order contributions in each channel, then these contain only the leading order term in the expansion of the thermal function \mathcal{G}_0 , *i.e.*, at order y^0 . The explicit expressions are

$$\Pi_D^{00} = -\frac{64\mu^4}{45\omega^4} y^4 \mathcal{G}_0 = -\frac{4q^4 v_F^4}{45\omega^4} \mathcal{G}_0, \tag{95}$$

$$\Pi_D^{jj} = -\frac{8\mu^2 v_F^2}{9\omega^2} y^2 \mathcal{G}_0 = -\frac{2q^2 v_F^4}{9\omega^2} \mathcal{G}_0, \tag{96}$$

$$\Pi_S^{00} = -v_F^2 \mathcal{G}_0, \tag{97}$$

$$\Pi_S^{jj} = -\frac{4\mu^2}{\omega^2} y^2 \mathcal{G}_0 = -\frac{q^2 v_F^2}{\omega^2} \mathcal{G}_0. \tag{98}$$

The last equalities in these expressions make it clear that the expansion, which was initially carried out with respect to the parameter q/k_F maps onto the expansion in v_F . It is seen that the vector current polarization tensors are of order $O(v_F^{\frac{1}{2}})$ while the axial vector polarization tensors are of order $O(v_F^2)$. The perturbative results (95) and (96) are in good agreement with the ones derived recently in the context of vector neutrino emission [31, 36, 37]. Similarly, the perturbative expressions in the spin channel (97) and (98) are in agreement with the original results derived in the context of the axial vector neutrino emission [36, 48–50].

B. Numerical results for response functions

Figures 1 and 2 show the dependence of the real and imaginary parts of the density and spin response functions, respectively, on the transferred energy for fixed three-momentum transfer. The zero temperature gap is fixed at $\Delta(0) = 1$ MeV and $T_c = \Delta(0)/1.76$. The lowest order Landau parameter is set $v_{\text{ph}}^D = -0.5$ for density perturbations and $v_{\text{ph}}^S = 0.5$ for spin perturbations (these correspond to the values computed in Ref. [33]). The frequency and momentum transfer are normalized to the threshold frequency $2\Delta(T)$. The response function in

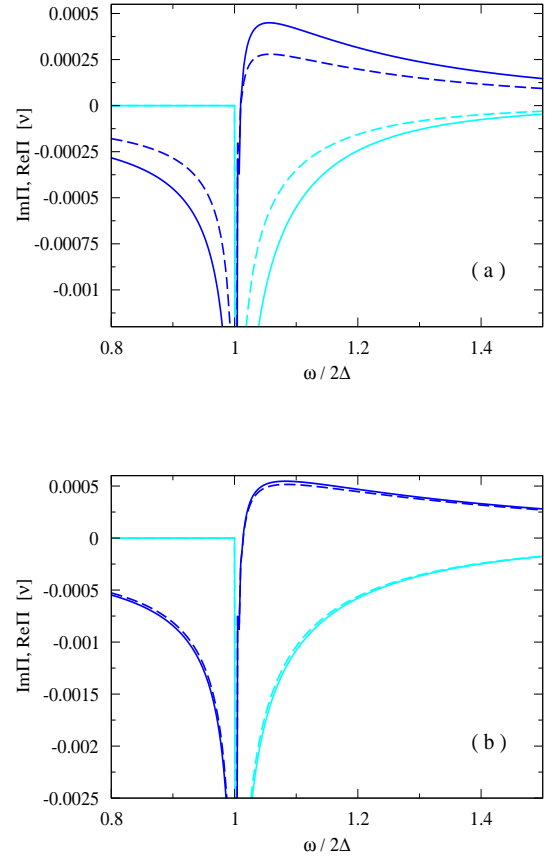


Figure 1: (Color online) Numerical (solid lines) and perturbative (dashed lines) results for the imaginary (heavy, blue line) and the real (light, cyan line) parts of the (a) density response function Π_{00}^D and (b) the density-current response function Π_{jj}^D normalized to the density of states ν in units fm^{-2} . The energy transfer ω is in units of $2\Delta(T)$. The temperature is fixed at $0.5T_c$ with pairing gap $\Delta = 1.0$ MeV. The ratio of momentum transfer and Fermi momentum is kept fixed at $q/k_F = 0.01$ and the Fermi momentum is set to $k_F = 1.0 \text{ fm}^{-1}$, which translates to the density $n = 0.221n_0$.

the negative energy range can be obtained from the relations $\text{Re}\Pi^{D/S}(-\omega) = \text{Re}\Pi^{D/S}(\omega)$ and $\text{Im}\Pi^{D/S}(-\omega) = -\text{Im}\Pi^{D/S}(\omega)$. The numerical method of computing the response functions exactly is described in appendix ??.

Our comparison of the perturbative analytical results with the exact numerical ones shows that (i) for the density response the higher-order corrections shift the imaginary part to higher frequencies, *i.e.*, for a fixed frequency the imaginary part is larger; the real parts are correspondingly larger as well. (ii) For the density current response the perturbative and exact results match to a high accuracy; (iii) for the spin-current response both results match again to a high accuracy; (iv) for the spin-density response small deviations are observed close to the threshold; the imaginary part is again shifted to higher frequencies. Note that in each case the imaginary

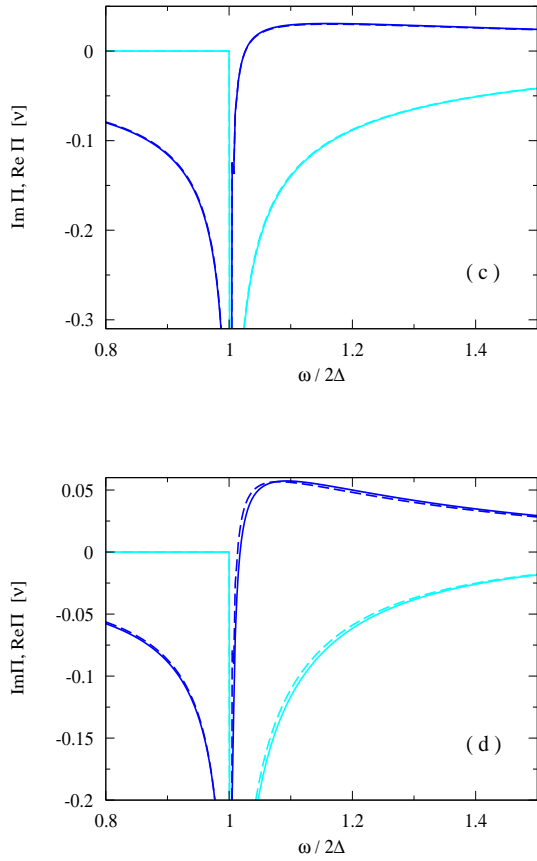


Figure 2: (Color online) The same as in Fig. 1, but for (c) the spin-current response function Π_{00}^S and (d) for the spin-density response function Π_{jj}^S (d).

parts are identically zero below the threshold for pair breaking process $2\Delta(T)$.

The density response function can be compared to the one derived in a previous paper [22]. As shown above, the first non-vanishing contribution arises from the term Π_{D4}^{00} and not from Π_{D2}^{00} as in Ref. [22], where $\Pi_{D2}^{00} \neq 0$. Consequently, the numerical values of the real and imaginary parts are roughly by an order of magnitude smaller. Nevertheless, the dependence of the real and imaginary parts of the polarization tensor on the frequency shows essentially the same behavior. The difference between the present results and that of Ref. [22] can be understood as follows. We note that the general form of the density response function in [22], Eq. (18) and the definitions of the elementary loops, Eqs. (19) to (22), are the same. The difference arises at the level of the loops \mathcal{A} , \mathcal{B} , and \mathcal{C} given by Eq. (25) to (27) of [22]. The most general form of the first loop, upon substitution of Bogolyubov amplitudes in Eqs. (19) and (21) of Ref. [22] is given by

$$\mathcal{A}(q) = \int \frac{d^3p}{(2\pi)^3} [(\epsilon + \epsilon')(\epsilon\epsilon' - \xi\xi' + \Delta^2) + \omega(\xi'\epsilon - \xi\epsilon')] \mathcal{G} \quad (99)$$

with the short-hand notations $\xi = \xi_{\mathbf{p}-\mathbf{q}/2}$, $\xi' = \xi_{\mathbf{p}+\mathbf{q}/2}$

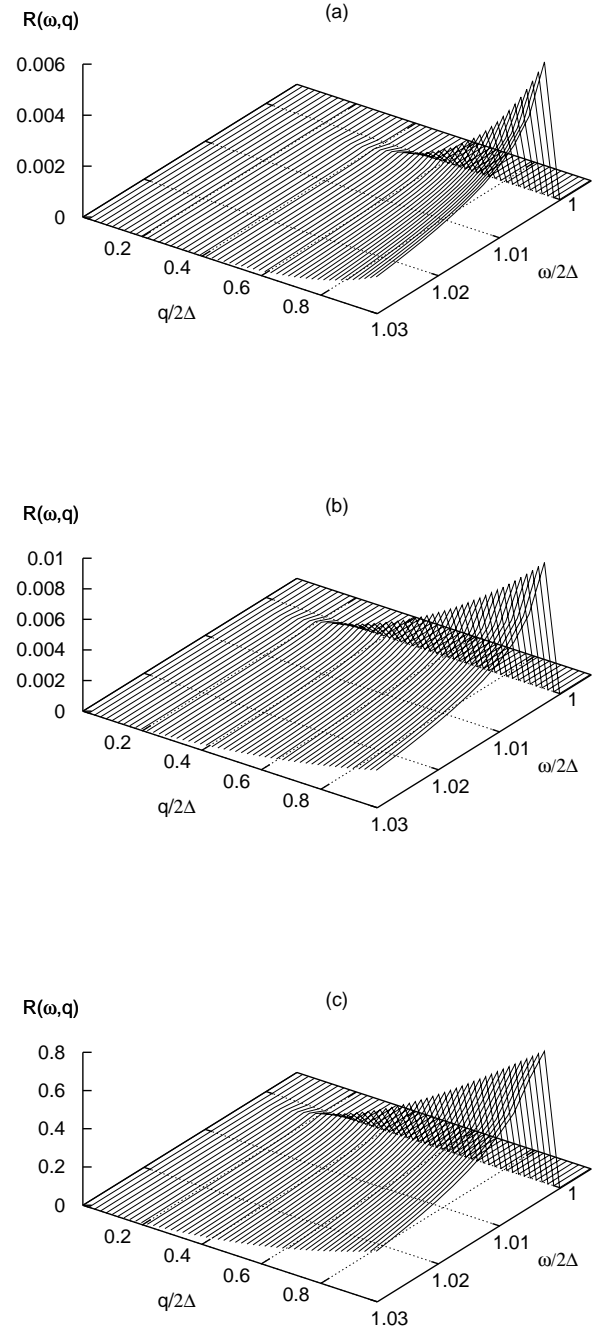


Figure 3: (Color online) The spectral function of (a) the density fluctuation, (b) current fluctuations and (c) spin-density fluctuations as a function of the energy transfer ω and of momentum transfer in units of $2\Delta(T)$ at $T = 0.5T_c$ and $k_F = 1 \text{ fm}^{-1}$, which corresponds to density $0.211 n_0$, where $n_0 = 0.16 \text{ fm}^{-3}$ is the nuclear saturation density.

and $\epsilon = \sqrt{\xi^2 + \Delta^2}$, $\epsilon' = \sqrt{(\xi')^2 + \Delta^2}$ and

$$\mathcal{G} = \frac{1}{2\epsilon\epsilon'} \left[\frac{1 - f(\epsilon) - f(\epsilon')}{\omega^2 - (\epsilon + \epsilon')^2} \right]. \quad (100)$$

We see that Eq. (25) of Ref. [22] does not contain the $\omega(\xi'\epsilon - \xi\epsilon')$ which vanishes manifestly in the limit $\mathbf{q} \rightarrow 0$, but is finite if $\mathbf{q} \neq 0$. For the remaining \mathcal{B} and \mathcal{C} loops we obtain

$$\mathcal{B}(q) = 2\Delta \int \frac{d^3p}{(2\pi)^3} [\omega\epsilon' + (\epsilon' + \epsilon)\xi'] \mathcal{G} \quad (101)$$

$$\mathcal{C}(q) = \int \frac{d^3p}{(2\pi)^3} \left\{ \frac{1 - 2f(\epsilon)}{2\epsilon} - [(\epsilon + \epsilon')(\epsilon\epsilon' + \xi\xi' + \Delta^2) - \omega(\xi\epsilon' + \xi'\epsilon)] \mathcal{G} \right\} \quad (102)$$

and we see that the terms $(\epsilon' + \epsilon)\xi'$ and $-\omega(\xi\epsilon' + \xi'\epsilon)$ are missing in Eqs. (26) and (27) of Ref. [22]. Both terms that were dropped vanish in the limit $\mathbf{q} \rightarrow 0$, because they are odd in ξ , while after changing the integration measure according to Eq. (A24), we obtain integrals over symmetrical in ξ limits. Thus, we conclude that, the discrepancy between the present treatment and that of Ref. [22] originates from incomplete expressions in Eqs. (25)-(27) of the latter work.

V. SPECTRAL FUNCTIONS AND COLLECTIVE MODES

The knowledge of the response functions allows us to construct an effective theory of excitations in the nuclear medium. Their full (interacting) propagator is completely determined by their spectral function, which in each channel is defined via the imaginary part of the polarization as $R(\omega, \mathbf{q}) = -2\text{Im}\Pi(\omega, \mathbf{q})$. For example, in the density channel, using Eq. (51), one finds

$$R(\omega, \mathbf{q}) = - \frac{2(v_{\text{ph}}^D)^{-2} \text{Im}P(\omega, \mathbf{q})}{\left[(v_{\text{ph}}^D)^{-1} - \text{Re}P(\omega, \mathbf{q}) \right]^2 + \text{Im}P(\omega, \mathbf{q})^2}, \quad (103)$$

where $P(\omega, \mathbf{q}) = \mathcal{Q}^+(\omega, \mathbf{q})/\mathcal{C}(\omega, \mathbf{q})$. Similar relations hold for other excitation channels (*i.e.*, current-density, spin-current and spin-density). Above the threshold $\omega > 2\Delta(T)$ non-zero imaginary part implies that the collective excitations have finite life-time, *i.e.*, are not perfect quasiparticles. Nevertheless, in the limit where the imaginary part is small one can approximate the spectral function as

$$R(\omega, \mathbf{q}) = 2\pi Z(\mathbf{q})\delta((v_{\text{ph}}^D)^{-1} - \text{Re}P(\omega, \mathbf{q})) + R_{\text{reg}}(\omega, \mathbf{q}), \quad (104)$$

where $R_{\text{reg}}(\omega, \mathbf{q})$ is the regular (*i.e.* smooth) part of the spectral functions and $Z(\mathbf{q})$ is the wave-function renormalization. The dispersion relation of the excitations is

given by the solution $\omega(\mathbf{q})$ of the equation

$$1 - v_{\text{ph}}^D \text{Re}P(\omega, \mathbf{q}) = 0. \quad (105)$$

Figure 3 shows the dependence of the spectral functions for density [Fig. 3(a)], current [Fig. 3(b)], and spin-density [Fig. 3(c)] fluctuations on the energy and momentum transfer. The spectral functions have a Breit-Wigner form, therefore the location of their maxima is controlled by the real parts of the response functions, whereas their widths by the imaginary parts. In the case of density fluctuations the imaginary component of the polarization tensor has a power-law ($\propto q^4$) behavior for fixed energy transfer, as is explicit from the analytical form (95). At fixed momentum transfer the spectral function has a threshold due to the proportionality $\mathcal{G}_0 \propto \theta(\omega - 2\Delta)$. At low-momentum transfer the main contribution to the spectral function comes from the vicinity of the pair breaking threshold ($\omega \sim 2\Delta$); for large momentum transfers, modes away from the energy threshold become important. The qualitative features seen in the spectral function of the density response are seen also for the current response; some quantitative differences arise because now, for fixed energy transfer, the imaginary part scales as $\propto q^2$, *c.f.* Eq. (96). Consequently, the low-momentum contributions are only weakly suppressed and the maximum of the spectral function is numerically larger. The response functions associated with spin perturbations appear at order v_F^2 , therefore their absolute scale is larger than that for the density and current-density responses, which scale as v_F^4 . It has the same functional dependence on the momentum and energy transfer as the density-current response [see Eq. (98)] and differs only by the numerical pre-factor and the v_F^2 dependence. For small momentum transfers the main contribution to the spectral function comes from the region near the threshold. Note that the spin-current response, to leading order, is independent of the momentum transfer, therefore the two-dimensional form given in Fig. 2 (c) is sufficient. Its dependence on the frequency reflects the dependence of the function \mathcal{G}_0 , *c.f.* Eq. (97).

From the spectral functions we can extract the quasi-particle spectra of the collective excitations. These can be defined by the poles of the spectral function when $\text{Im}P(\omega, \mathbf{q}) = 0$, *i.e.*, by the condition (105). We start by setting the parameters characterizing the superfluid state to their relevant scales and by studying the nature of the modes as a function of the particle-hole interaction v_{ph} . The stability of the normal Fermi-liquid state constrains $v_{\text{ph}} > -1$ (note that we work at leading order in the expansion of Landau parameters in spherical harmonics). The numerical solutions of Eq. (105) for the density and spin excitations are shown in Fig. 4 for $-1 \leq v_{\text{ph}} \leq 2$ and fixed $k_F = 1 \text{ fm}^{-1}$, $T/T_c = 0.5$ with $\Delta = 1 \text{ MeV}$. For positive values of the particle-hole interaction the modes appear in the domain $\omega/2\Delta > 1$, where $\text{Im}P(\omega, \mathbf{q}) \neq 0$, *i.e.*, they represent damped (diffusive) modes of oscillations of density and spin-density, respectively, associated with the pair-breaking processes. For negative values of

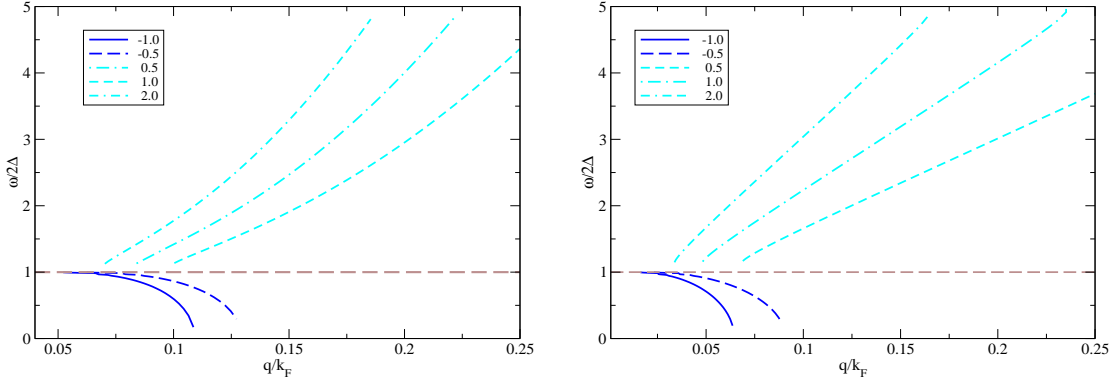


Figure 4: (Color online) Dispersion relations of collective excitations for density (left panel) and spin density (right panel) perturbations for the values of the particle-hole interaction v_{ph} shown in each panel for $k_F = 1 \text{ fm}^{-1}$ and $T/T_c = 0.5$. The heavy lines (blue online) correspond to undamped excitonic modes, the light lines (cyan online) correspond to diffusive damped pair-breaking modes.

the particle-hole interaction, the modes exist in the domain $\omega/2\Delta \leq 1$, where the pair-breaking part of the $\text{Im}P(\omega, \mathbf{q})$ vanishes; therefore the modes represent undamped oscillations of density and spin-density around their average values. These modes are “exitonic” as they correspond to bound pairs of particles and holes. The

Table I: The values of the coefficients in the fit formula (106) for several values of the particle-hole interaction in the density (upper part) and spin (lower part) channels. The remaining parameters are fixed to their characteristic values $k_F = 1 \text{ fm}^{-1}$, $\Delta = 1 \text{ MeV}$, and $m^*/m = 1$. The interactions are given in units of the density of states $\nu(k_F)$.

v_{ph}	a	b	c	d
-1	0.817879	88.4029	-11411.2	
-0.5	0.849483	53.7703	-5210.88	
0.5	0.600277	80.4847	115.199	
1	0.586293	57.3376	49.0417	
2	0.584029	116.109	193.221	
-1	1.02616	-84.0295	2216.43	-7449470.
-0.5	1.02487	-39.6023	-568.605	-844334.
0.5	0.885174	83.0049	-922.6	4886.17
1	0.928416	154.6	-2912.19	26000.1
2	0.924387	313.859	-12031.8	218234.

spectra in each case can be accurately fitted by the polynomial of the form

$$\tilde{\omega}(q) = a + b\tilde{q}^2 + c\tilde{q}^4 + d\tilde{q}^6, \quad (106)$$

where in the case of density perturbations accurate results are obtained with only three parameters ($d = 0$). Here we defined dimensionless quantities $\tilde{\omega} = \omega/2\Delta$ and $\tilde{q} = q/k_F$. The fitted values of the parameters for the results shown in Fig. 4 and are given in Table I.

Next we consider a specific microscopic calculation [33], which provides us with the density dependence

Table II: The same as in Table I, but for the density-dependent v_{ph} interactions taken from Ref. [33]. The entries are the Fermi wave vector, the values of the coefficients in the fit formula (106), and the range of momentum transfers Δq in units of k_F .

k_F	v_{ph}	a	b	c	$k_F^{-1} \Delta q$
1.0	-0.45	0.941366	2.69439	-34.0444	(0.197; 0.29)
	0.41	0.518545	12.4875	8.8972	(0.223; 0.3)
1.2	-0.43	0.896992	12.9105	-447.747	(0.111; 0.22)
	0.40	0.6465	37.092	-197.621	(0.127; 0.3)
1.4	-0.41	0.901629	67.8547	-12952.2	(0.047; 0.098)
	0.40	1.17054	84.3504	-488.556	(0.054; 0.3)
1.6	-0.36	0.894476	702.973	-1283650	(0.015; 0.031)
	0.39	1.15211	859.001	-49727.6	(0.018; 0.08)

of the parameters of the neutron superfluid *and* the associated values of the leading-order Landau parameters in the particle-hole channel. We solved Eq. (105) in the density and spin channels for each density and subsequently fitted the spectra with the formula (106). The results are displayed in Table II; some of the characteristics of the superfluid are shown in Table III. The density excitations exist below the pair-breaking threshold, *i.e.*, represent undamped excitonic modes. Conversely, because v_{ph} changes the sign in the spin channel, the spin excitations represent diffusive modes with finite damping. Note that each of these modes exist within some finite interval Δq of momentum transfers. The lower bound arises because perturbations that are sufficiently large to excite a mode arise at some *finite value* of q . The upper bound in most cases is the consequence of the use of perturbative response functions, whose validity breaks down for large momentum transfers $q/k_F \sim 0.3$; in some cases the upper bounds are associated with the disappearance

of the solutions from the search domain.

VI. SPECIFIC HEAT

The specific heat contribution arising from the collective modes in the neutron star crust has recently attracted recently attention in the context of non-spherical phases [41]. These modes at not too low temperatures can dominate the specific heat provided by the degenerate, ultra-relativistic electron gas. Below we shall examine the contribution of the collective modes discussed in the previous section to the specific heat of a superfluid neutron star crust.

The entropy of a collective bosonic mode is given by

$$S = 2k_B \sum_{\mathbf{q}} [(1 + g_{\mathbf{q}}) \ln(1 + g_{\mathbf{q}}) + g_{\mathbf{q}} \ln g_{\mathbf{q}}], \quad (107)$$

where $g_{\mathbf{q}} = [\exp(\omega_{\mathbf{q}}/T) - 1]^{-1}$ is the Bose distribution function of collective excitations with the spectrum $\omega_{\mathbf{q}}$. The specific heat is then given by

$$c_V = k_B T \frac{dS}{dT} = k_B \sum_{\mathbf{q}} \frac{\omega_{\mathbf{q}}}{T} \frac{\partial g_{\mathbf{q}}}{\partial T}. \quad (108)$$

For a collective (acoustic) mode with linear spectrum $\omega = u|\mathbf{q}|$, where u is the sound velocity, Eq. (108) can be integrated [55]

$$c_V^{(a)} = \frac{2\pi^2 k_B^4 T^3}{15(\hbar u)^3}. \quad (109)$$

An acoustic mode, in a compact star setting, is associated with the nuclear lattice in the crust, where phonons contribute to the specific heat below the melting temperature of the crust $\sim 10^9$ K. At low temperatures the superfluid supports the Bogolyubov-Anderson (BA) mode with the velocity

$$v_F^{\text{BA}} = \frac{v_F}{\sqrt{3}} (1 + v_{\text{ph}}^D)^{1/2}. \quad (110)$$

where $v_F = \hbar k_F / m^*$ is the (effective) Fermi velocity. The dispersion relation (110) does not contain temperature corrections. In the following we will ignore the damping of the BA mode and extrapolate the result (110) to higher temperatures. Apart from these two collective modes, the main contribution to the specific heat of matter is due to the electrons which, in a first approximation, can be treated as a uniform ultra-relativistic ideal Fermi gas. At low temperatures their specific heat is then given by

$$c_V^{(e)} = \frac{k_B^2 \mu_e^2 T}{3(\hbar c)^3}, \quad (111)$$

where μ_e is the electron chemical potential.

Table III compares the various contributions to the specific heat of matter at subnuclear densities. The temperature at each density corresponds to $T = 0.5T_c$, with

Table III: Density and wave-vector dependence of the specific heat of various components in neutron matter and the crust of a neutron star at $T = 0.5T_c$. Tabulated are the net density of matter n_n [fm⁻³], the neutron wave-vector k_F [fm⁻¹], the neutron effective mass in units of bare mass, the pairing gap Δ [MeV], the electron wave-vector k_{Fe} [fm⁻¹], assuming that the electron number density $n_e = 0.023n_n$, the specific heats of electron gas $c_V^{(e)}$, Bogolyubov-Anderson phonons $c_V^{(\text{BA})}$, pair-breaking density fluctuations $c_V^{(\rho)}$, pair-breaking spin fluctuations $c_V^{(\sigma)}$ in units of 10^{18} erg cm⁻³ K⁻¹.

n_n	k_F	m^*	Δ	k_{Fe}	$c_V^{(e)}$	$c_V^{(\text{BA})}$	$c_V^{(\rho)}$	$c_V^{(\sigma)}$
0.034	1.00	0.94	3.09	0.29	16.6	26.419	2.479	0.291
0.058	1.20	0.92	2.44	3.42	18.9	7.611	3.508	0.079
0.093	1.40	0.88	1.41	3.99	14.8	1.003	0.008	0.004
0.138	1.60	0.84	0.57	0.45	7.8	0.045	0.012	0.000

$T_c = \Delta/1.76$. The contribution of the BA mode, c_V^{BA} is computed from Eqs. (109) and (110), the contribution of electrons from Eq. (111) assuming $n_e = 0.023n_n$, where n_e and n_n are the electron and neutron number densities. The contributions from density and spin pair-breaking contributions, $c_V^{(\rho)}$ and $c_V^{(\sigma)}$ are computed through the numerical integration of Eq. (108) with the collective mode spectrum given by Eq. (106). The coefficients a , b and c in Eq. (106) for the density fluctuations and the spin fluctuations, as well as the integration limits in Eq. (108) are tabulated in Table II (the coefficient $d = 0$ in all cases). It is seen that the density fluctuations considerably contribute to the net specific heat of matter for lower densities (wave-vectors), while the spin-fluctuations are negligible at $T/T_c = 0.5$. The result of for the BA mode should be taken as suggestive, because we neglected the temperature correction to the dispersion relation and the possible damping of this mode.

The temperature dependence of the specific heat due to the pair-breaking modes and the specific heat of electron gas is shown in Fig. 5 for $k_F = 1$ fm⁻¹. The electron specific heat is linear in temperature, whereas the specific heat of the pair-breaking fluctuations has a power law behavior, which is close to the T^3 law characteristic for linear in q spectra. The difference reflects the non-linearity of the spectrum (106). We have assumed that the temperature dependence of the coefficients a , b , and c can be neglected in a first approximation, *i.e.*, the spectrum of collective excitations is assumed to be independent of temperature. This assumption is validated by the insensitivity of the maxima of the spectral functions to the temperature variations (see Fig. 3) which were compared at $T/T_c = 0.5$ and 0.9 .

VII. CONCLUSIONS

In this work we studied the response functions of a single component pair-correlated baryonic matter to density, spin and their current perturbations in the low-

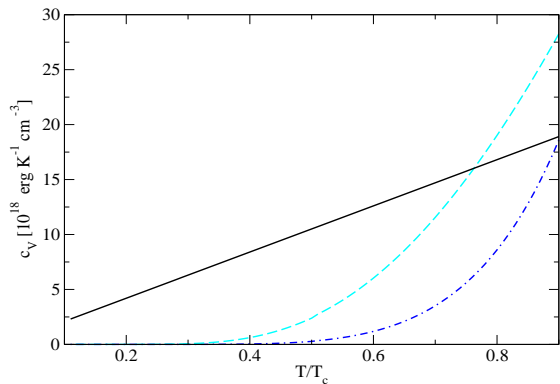


Figure 5: (Color online) Dependence of the specific heats due to electrons (solid line) and pair-breaking density (dashed line) and spin fluctuations (dash-dotted line) on the reduced temperature T/T_c for $k_F = 1 \text{ fm}^{-1}$.

temperature regime. These results should be relevant for the description of both the dynamical and thermodynamical properties of baryonic matter at low densities, *i.e.*, the densities where the baryons form an S -wave superfluid. It was observed that the expansions in the parameters q/k_F and $v_F q/\omega$ lead essentially to the same perturbative results, which in turn can be interpreted as an expansion in the parameter $v_F \ll 1$. We have applied an exact numerical method to evaluate the response functions and to validate the perturbative approximation in the domain of its convergence. We further derived the dispersion relations of the collective excitations of density and spin-density perturbations. For positive values of the particle-hole interactions these correspond to weakly damped diffusive excitations, whereas for negative values - to undamped excitonic modes.

The spectral functions presented above can be modified in a number of ways. As noted in the Introduction the multi-loop processes were found to be important for the neutrino emission and they could additionally contribute to the spectral functions in the kinematical domain where two-particle-two-hole excitations are important. Furthermore, higher order Landau parameters, if included into driving interactions in the particle-particle and particle-hole channels may require some renormalization of the spectra, see Refs. [51–54].

The application of the formalism to compute the specific heat of the matter expected in neutron star crusts shows that the contribution of the collective pair-breaking excitations can be a significant part of the net specific heat of matter. For some density parameters and not too low temperatures the combined contribution from superfluid modes of neutron fluid can be larger than the specific heat stored in the degenerate electron gas.

Acknowledgment

This work was supported by the Deutsche Forschungsgemeinschaft Grant No. SE 1836/1-2 (JK), the HGS-HIRE graduate program (JK), and by GSI (AS).

Appendix A: Solving the equations for the vertices

The bare vertices given by Eq. (4) are diagonal in spin space. Likewise, the particle and hole vertices are diagonal in spin space, *i.e.*, $\hat{\Gamma}_1 = \Gamma_1 \hat{1}_2$ and $\hat{\Gamma}_4 = \Gamma_4 \hat{1}_2$. The anomalous vertices are proportional to the second Pauli matrix, $\hat{\Gamma}_2 = \Gamma_2 i\sigma_2$ and $\hat{\Gamma}_3 = \Gamma_3 i\sigma_2$. The equation for the hole vertex Γ_4 can be obtained from the equation for the particle vertex Γ_1 by interchanging particle and hole lines. To account for this property one can introduce, following Ref. [27], an operator $\hat{\mathcal{P}}$ to revert the direction of ingoing and outgoing momenta and to exchange the spin indices simultaneously, when acting on a vertex function. The explicit action of this operator is

$$\mathcal{P}\Gamma_{4,\alpha\beta} = \sigma_y \Gamma_{4,\alpha\beta}^* \sigma_y = \mathcal{T}\Gamma_{1,\alpha\beta}, \quad (\text{A1})$$

whereby \mathcal{T} is the time-reversal operator, *i.e.*, it is equal to $+1$ for vertices which are even under time reversal operation and -1 for vertices which are odd under this transformation. By considering the action of the operator $\hat{\mathcal{P}}$ on the bare vertices one finds that scalar vertices, *e.g.*, $\Gamma_0^D = 1$ and $\Gamma_0^S = \boldsymbol{\sigma}\boldsymbol{v}$ do not change their sign, while vector vertices like $\Gamma_0^D = \boldsymbol{v}$ or $\Gamma_0^S = \boldsymbol{\sigma}$ gain an additional minus sign. Furthermore, we note that the equations for Γ_2 and Γ_3 are adjoint to each other. Formally, one can cast this property into the equation

$$\hat{\Gamma} = -\hat{\Gamma}_2 = \hat{\Gamma}_3^+. \quad (\text{A2})$$

Note that the full current vertices can depend on any external momentum involved in the problem, therefore they need to be decomposed in components along the vectors \boldsymbol{v} and \boldsymbol{q} . Thus, the most general Ansatz for the density current vertices is

$$\Gamma^D = \Gamma_v^D \boldsymbol{n}_v + \Gamma_q^D \boldsymbol{n}_q, \quad (\text{A3})$$

$$\tilde{\Gamma}^D = \tilde{\Gamma}_q^D \boldsymbol{n}_q, \quad (\text{A4})$$

where the subscripts on the unit vector \boldsymbol{n} refer to the vector defining its direction. The coefficients $\Gamma_{v,q}^D$ are normalized such that $\Gamma^D \boldsymbol{n}_v = \boldsymbol{v}_F$, *i.e.*, the coefficient Γ^D is simply the modulus of the Fermi velocity. Similar to Eqs. (A3) and (A4) decompositions holds for spin-current vertices.

The solution of the system (36) to (39) is simplified if one takes into account the identities [27, 28]

$$GG^-(\boldsymbol{v}, \omega, \boldsymbol{q}) = G^-G(\boldsymbol{v}, \omega, \boldsymbol{q}), \quad (\text{A5})$$

$$G^-F(\boldsymbol{v}, \omega, \boldsymbol{q}) = -FG^-(\boldsymbol{v}, \omega, \boldsymbol{q}), \quad (\text{A6})$$

$$GF(\boldsymbol{v}, \omega, \boldsymbol{q}) = -FG(\boldsymbol{v}, \omega, \boldsymbol{q}), \quad (\text{A7})$$

$$G^-G^-(\boldsymbol{v}, \omega, \boldsymbol{q}) = GG(\boldsymbol{v}, -\omega, \boldsymbol{q}), \quad (\text{A8})$$

where the products of the Green's functions refer to their convolutions defined as z

$$X_+ X'_- = \nu T \sum_{n=-\infty}^{\infty} \int_{-\infty}^{\infty} d\xi_p X \left(ip_n + i\omega_m, \mathbf{p} + \frac{\mathbf{q}}{2} \right) \times X' \left(ip_n, \mathbf{p} - \frac{\mathbf{q}}{2} \right), \quad (\text{A9})$$

where $X_{\pm} \in \{G_{\pm}, G_{\pm}^-, F_{\pm}, F_{\pm}^+\}$. The solution contains the following linear combinations of the convolutions [24, 27, 28]:

$$A(\hat{\mathcal{P}}) = G_+ G_- - F_+ F_- \hat{\mathcal{P}}, \quad (\text{A10})$$

$$B = G_+ F_- - F_+ G_-, \quad (\text{A11})$$

$$C = G_+ G_- + F_+ F_- - v_{\text{pp}}^{-1}, \quad (\text{A12})$$

$$D(\hat{\mathcal{P}}) = -G_+ F_- - F_+ G_- \hat{\mathcal{P}}. \quad (\text{A13})$$

We take the matrix structure of vertices and propagators into account and use the relations (A1) and (A2) to cast the set of the four coupled integral equations into the following two equations for the new vertex functions

$$\Gamma^{D/S}(\mathbf{v}, \omega, \mathbf{q}) = \Gamma_0^{D/S}(\mathbf{v}, \omega, \mathbf{q}) + \int \frac{d\Omega'}{4\pi} V_{\text{ph}}^{D/S}(\mathbf{v}, \mathbf{v}') \times \left[A(\hat{\mathcal{P}}) \Gamma^{D/S}(\mathbf{v}', \omega, \mathbf{q}) + B \tilde{\Gamma}^{D/S}(\mathbf{v}', \omega, \mathbf{q}) \right], \quad (\text{A14})$$

$$\tilde{\Gamma}^{D/S}(\mathbf{v}', \omega, \mathbf{q}) = \int \frac{d\Omega'}{4\pi} V_{\text{pp}}^{D/S}(\mathbf{v}, \mathbf{v}') \times \left[(C + v_{\text{pp}}^{-1}) \tilde{\Gamma}^{D/S}(\mathbf{v}', \omega, \mathbf{q}) + D(\hat{\mathcal{P}}) \Gamma^{D/S}(\mathbf{v}', \omega, \mathbf{q}) \right]. \quad (\text{A15})$$

To write down the solutions of the integral equation we need the following angle averages of the loop functions

$$A(\hat{\mathcal{P}}) = \int \frac{d\Omega}{4\pi} A(\hat{\mathcal{P}}), \quad (\text{A16})$$

$$B = \int \frac{d\Omega}{4\pi} B, \quad (\text{A17})$$

$$C = \int \frac{d\Omega}{4\pi} C, \quad (\text{A18})$$

$$D(\hat{\mathcal{P}}) = \int \frac{d\Omega}{4\pi} D(\hat{\mathcal{P}}), \quad (\text{A19})$$

where $d\Omega = \sin\theta d\theta d\phi$. Furthermore, we need the angle averages of first moments of the loop functions with respect to the cosine of the angle enclosed by \mathbf{n}_v and \mathbf{n}_q , i.e., $x \equiv \mathbf{n}_q \cdot \mathbf{n}_v$, which we write as

$$\tilde{\mathcal{Y}} = \int \frac{d\Omega}{4\pi} \tilde{Y}, \quad (\text{A20})$$

where

$$\tilde{Y} = x \nu T \sum_{n=-\infty}^{\infty} \int_{-\infty}^{\infty} d\xi_p X \left(ip_n + i\omega_m, \mathbf{p} + \frac{\mathbf{q}}{2} \right) \times X' \left(ip_n, \mathbf{p} - \frac{\mathbf{q}}{2} \right). \quad (\text{A21})$$

We also define the auxiliary combination of the loops:

$$\mathcal{Q}^{\pm}(\omega, \mathbf{q}) = \mathcal{A}^{\pm}(\omega, \mathbf{q}) \mathcal{C}(\omega, \mathbf{q}) - \mathcal{B}(\omega, \mathbf{q}) \mathcal{D}^{\pm}(\omega, \mathbf{q}), \quad (\text{A22})$$

$$\tilde{\mathcal{Q}}^{\pm}(\omega, \mathbf{q}) = \tilde{\mathcal{A}}^{\pm}(\omega, \mathbf{q}) \mathcal{C}(\omega, \mathbf{q}) - \tilde{\mathcal{B}}(\omega, \mathbf{q}) \mathcal{D}^{\pm}(\omega, \mathbf{q}). \quad (\text{A23})$$

The computations of the phase-space integrals in Eqs. (A10) to (A13) can be simplified [28], because each loop can be written as a product of some thermal function and a pre-factor that depends only on the quantities ω and $\mathbf{q} \cdot \mathbf{v}_F$. To carry out the phase-space integrations we first change the integration measure:

$$\int \frac{d^3 p}{(2\pi)^3} \simeq \nu \int \frac{d\Omega}{4\pi} \int_{-\infty}^{\infty} d\xi_p, \quad (\text{A24})$$

where we used the fact that at low temperatures the lower integration limit $-\mu/T \simeq -\infty$. For the sake of completeness we list the resulting expressions for the loops [27, 28]

$$\mathcal{A}^{\pm} = \nu \int \frac{d\Omega}{4\pi} \left\{ -\frac{1 \pm \hat{\mathcal{P}}}{2} \mathcal{G}(\mathbf{v}, \omega, \mathbf{q}) + \frac{\mathbf{q}\mathbf{v}}{\omega - \mathbf{q}\mathbf{v}} \left[\mathcal{G}(\mathbf{v}, \mathbf{q}\mathbf{v}, \mathbf{q}) - \mathcal{G}(\mathbf{v}, \omega, \mathbf{q}) \right] \right\}, \quad (\text{A25})$$

$$\mathcal{B} = -\nu \int \frac{d\Omega}{4\pi} \frac{\omega + \mathbf{q}\mathbf{v}}{2\Delta} \mathcal{G}(\mathbf{v}, \omega, \mathbf{q}), \quad (\text{A26})$$

$$\mathcal{C} = \nu \int \frac{d\Omega}{4\pi} \frac{\omega^2 - (\mathbf{q}\mathbf{v})^2}{4\Delta^2} \mathcal{G}(\mathbf{v}, \omega, \mathbf{q}), \quad (\text{A27})$$

$$\mathcal{D}^{\pm} = \nu \int \frac{d\Omega}{4\pi} \left[\frac{\omega + \mathbf{q}\mathbf{v}}{4\Delta} + \frac{\omega - \mathbf{q}\mathbf{v}}{4\Delta} \hat{\mathcal{P}} \right] \mathcal{G}(\mathbf{v}, \omega, \mathbf{q}), \quad (\text{A28})$$

where the thermal function is given by

$$\mathcal{G}(\mathbf{v}, \omega, \mathbf{q}) = \Delta^2 \int_{-\infty}^{+\infty} d\xi_p \times \left[\frac{\epsilon_+ - \epsilon_-}{\epsilon_+ \epsilon_-} \frac{f(\epsilon_-) - f(\epsilon_+)}{\omega^2 - (\epsilon_+ - \epsilon_-)^2 + i\eta} - \frac{\epsilon_+ + \epsilon_-}{\epsilon_+ \epsilon_-} \frac{1 - f(\epsilon_-) - f(\epsilon_+)}{\omega^2 - (\epsilon_+ + \epsilon_-)^2 + i\eta} \right], \quad (\text{A29})$$

where $f(x) = \{\exp[(x - \mu)/T] + 1\}^{-1}$ is the fermionic distribution function. In the following we focus on the pair-breaking part of Eq. (A29) given by

$$\mathcal{G}^{\text{pb}}(\mathbf{v}, \omega, \mathbf{q}) = -\Delta^2 \int_{-\infty}^{+\infty} d\xi_p \frac{(\epsilon_+ + \epsilon_-)}{\epsilon_+ \epsilon_-} \times \frac{1 - f(\epsilon_-) - f(\epsilon_+)}{\omega^2 - (\epsilon_+ + \epsilon_-)^2 + i\eta}, \quad (\text{A30})$$

which is the dominant part of the response in the low-temperature domain.

Appendix B: Thermal function

1. Analytical result

Here we determine the real and imaginary parts of the zeroth order coefficient in the expansion of the thermal function. The first step is to use the generalized Dirac identity

$$\int \frac{dz f(z)}{(z - \zeta + i\eta)^{n+1}} = \int \frac{dz f(z)}{(z - \zeta)^{n+1}} - i\pi \frac{(-1)^n}{n!} \int dz f(z) \frac{\partial^n}{\partial z^n} \delta(z - \zeta) \quad (\text{B1})$$

and to decompose the complex function at hand into real and imaginary parts. The imaginary part can be integrated analytically using the partial integration in the formula

$$\int_{\alpha}^{\beta} dz f(z) \delta^{(n)}(z - \zeta) = (-1)^n \left. \frac{\partial^n f(z)}{\partial z^n} \right|_{z=\zeta} \quad \forall \zeta \in [\alpha, \beta]. \quad (\text{B2})$$

Once the imaginary part is calculated, the real part can be obtained via the Kramers-Kronig relation

$$\text{Re} \phi(\omega) = \frac{1}{\pi} \int_{-\infty}^{+\infty} \frac{d\omega' \text{Im} \phi(\omega')}{\omega' - \omega}, \quad (\text{B3})$$

provided that the imaginary part decays faster than $1/\omega$ for large ω . The application of this procedure to the thermal function to leading order gives

$$\mathcal{G}_0^{\text{pb}} = -\Delta^2 \int_{-\infty}^{\infty} d\xi_p \frac{2 \tanh\left(\frac{\xi_p}{2T}\right)}{\epsilon_p(\omega^2 - 4\epsilon_p^2 + i\delta)}. \quad (\text{B4})$$

Next we compute the imaginary part and obtain

$$\begin{aligned} \text{Im} \mathcal{G}_0^{\text{pb}} &= \pi \Delta^2 \int_{-\infty}^{\infty} d\xi_p \frac{2 \tanh\left(\frac{\xi_p}{2T}\right)}{\epsilon_p} \delta(\omega^2 - 4\epsilon_p^2) \\ &= \frac{2\pi \Delta^2}{|\omega|} \frac{\tanh\left(\frac{\omega}{4T}\right)}{\sqrt{\omega^2 - 4\Delta^2}} \theta\left(\frac{\omega}{2} - \Delta\right). \end{aligned} \quad (\text{B5})$$

Note the threshold behavior enforced by the Heavyside function: Energy transfer is possible only for frequencies larger than the pair-breaking threshold 2Δ . Furthermore, the thermal function at this order is independent of the momentum transfer; this implies that the momentum-transfer dependence of the response functions is determined by the pre-factors of the loop functions [c.f. Eqs. (A25) to (A28)].

2. Numerical calculation of the thermal function

In this section we focus on the numerical calculation of the angle average of the thermal function, which is given

by

$$\begin{aligned} \mathcal{G}^{\text{pb}}(\mathbf{v}, \omega, \mathbf{q}) &= -\Delta^2 \int \frac{d^3 p}{(2\pi)^3} \frac{(\epsilon_+ + \epsilon_-)}{\epsilon_+ \epsilon_-} \\ &\times \frac{(1 - f(\epsilon_-) - f(\epsilon_+))}{(\omega^2 - (\epsilon_+ + \epsilon_-)^2 + i\eta)} \\ &= -2\Delta^2 \int_0^{2\pi} \frac{d\phi}{2\pi} \int_{-1}^{+1} \frac{dx}{2} \int_{\Delta}^{\infty} \frac{d\epsilon_p \epsilon_p}{\sqrt{\epsilon_p^2 - \Delta^2}} \frac{(\epsilon_+ + \epsilon_-)}{\epsilon_+ \epsilon_-} \\ &\times \frac{(1 - f(\epsilon_-) - f(\epsilon_+))}{(\omega^2 - (\epsilon_+ + \epsilon_-)^2 + i\eta)}. \end{aligned} \quad (\text{B6})$$

The factor of 2 in the second relation arises from the fact that the integrand is an even function of ξ_p and the integration can be restricted to the positive values of the argument. We have also replaced the integration over the paired spectrum by the integration over the unpaired spectrum by the integration over the paired spectrum by means of the relation $\xi_p d\xi_p = \epsilon_p d\epsilon_p$. The integral over the azimuthal angle is trivial, since the integrand is independent of ϕ . Further, after using the Dirac identity we obtain

$$\begin{aligned} \text{Im} \mathcal{G}^{\text{pb}}(\mathbf{v}, \omega, \mathbf{q}) &= 2\pi \Delta^2 \int_{-1}^{+1} \frac{dx}{2} \int_{\Delta}^{\infty} \frac{d\epsilon_p \epsilon_p}{\sqrt{\epsilon_p^2 - \Delta^2}} \frac{(\epsilon_+ + \epsilon_-)}{\epsilon_+ \epsilon_-} \\ &\times (1 - f(\epsilon_+) - f(\epsilon_-)) \delta\left(\omega^2 - (\epsilon_+ + \epsilon_-)^2\right). \end{aligned} \quad (\text{B7})$$

One of the integrations can be carried out with the help of the δ function. One finds

$$\begin{aligned} \text{Im} \mathcal{G}^{\text{pb}}(\mathbf{v}, \omega, \mathbf{q}) &= \frac{\pi \Delta^2}{2} \int_{\Delta}^{\infty} \frac{d\epsilon_p \epsilon_p}{\sqrt{\epsilon_p^2 - \Delta^2}} \\ &\times \sum_{x_1, x_2} \frac{(\epsilon_+ + \epsilon_-)}{\epsilon_+ \epsilon_-} \frac{[1 - f(\epsilon_+) - f(\epsilon_-)]}{|(\epsilon_+ + \epsilon_-)'|_{x=x_{1,2}}} \theta(1 - |x_{1,2}|). \end{aligned} \quad (\text{B8})$$

where $x_{1,2}$ are the solutions of the equation $\omega^2 - [\epsilon_+(x) + \epsilon_-(x)]^2 = 0$ and the prime denotes a derivative with respect to x ; its explicit form is given elsewhere [53]. Once the imaginary part is computed, the real part follows from the Kramers-Kronig relation. This completes our numerical procedure for computing the response functions. Each of the loops (A25) to (A28) can be computed by multiplying the numerical result for the thermal function by the appropriate pre-factor.

Appendix C: Comparison to Leggett's formalism

Here we compare the response functions derived above with the results obtained in the Leggett formalism [28, 35] and establish the correspondence between the two. The full (effective) normal vertices in the Leggett's formalism [28] are defined as symmetrical and anti-symmetrical combinations of the particle τ and hole τ^h

vertices

$$\tau^+ = \frac{1}{2}(\tau + \tau^h), \quad \tau^- = \frac{1}{2}(\tau - \tau^h). \quad (\text{C1})$$

If $\tau = \pm\tau^h$, *i.e.*, the vertices have odd or even parity under transformations which convert particles into holes, then one of the linear combinations (C1) vanishes. The bare vertices are defined analogously

$$\xi^+ = \frac{1}{2}(\xi + \xi^h), \quad \xi^- = \frac{1}{2}(\xi - \xi^h). \quad (\text{C2})$$

The anomalous vertex is denoted by $\tilde{\tau}$. With these definitions the integral equations for the full vertices are

$$\begin{aligned} & \left[1 - \int \frac{d\Omega'}{4\pi} V_{\text{pp}}^{D/S}(\mathbf{v}\mathbf{v}') A_0 \right. \\ & \left. + \int \frac{d\Omega'}{4\pi} V_{\text{pp}}^{D/S}(\mathbf{v}\mathbf{v}') \frac{\omega^2 - (\mathbf{q}\mathbf{v}')^2}{2\Delta^2} \lambda(\mathbf{v}') \right] \tilde{\tau} \\ & + \int \frac{d\Omega'}{4\pi} V_{\text{pp}}^{D/S}(\mathbf{v}\mathbf{v}') \frac{\mathbf{q}\mathbf{v}'}{\Delta} \lambda(\mathbf{v}') \tau^- \\ & - \int \frac{d\Omega'}{4\pi} V_{\text{pp}}^{D/S}(\mathbf{v}\mathbf{v}') \frac{\omega}{\Delta} \lambda(\mathbf{v}') \tau^+ = 0, \end{aligned} \quad (\text{C3})$$

$$\begin{aligned} & \int \frac{d\Omega'}{4\pi} V_{\text{ph}}^{D/S}(\mathbf{v}\mathbf{v}') \frac{\mathbf{q}\mathbf{v}'}{\Delta} \lambda(\mathbf{v}') \tilde{\tau} \\ & + \left[1 - \int \frac{d\Omega'}{4\pi} V_{\text{ph}}^{D/S}(\mathbf{v}\mathbf{v}') \kappa(\mathbf{v}') \right] \tau^- \\ & + \int \frac{d\Omega'}{4\pi} V_{\text{ph}}^{D/S}(\mathbf{v}\mathbf{v}') \frac{\omega}{\mathbf{q}\mathbf{v}'} \kappa(\mathbf{v}') \tau^+ = \xi^-, \quad (\text{C4}) \\ & - \int \frac{d\Omega'}{4\pi} V_{\text{ph}}^{D/S}(\mathbf{v}\mathbf{v}') \frac{\omega}{\Delta} \lambda(\mathbf{v}') \tilde{\tau} \\ & + \int \frac{d\Omega'}{4\pi} V_{\text{ph}}^{D/S}(\mathbf{v}\mathbf{v}') \frac{\omega}{\mathbf{q}\mathbf{v}'} \kappa(\mathbf{v}') \tau^- \\ & + \left[1 - \int \frac{d\Omega'}{4\pi} V_{\text{ph}}^{D/S}(\mathbf{v}\mathbf{v}') (\kappa(\mathbf{v}') - 2\lambda(\mathbf{v}')) \right] \tau^+ = \xi^+, \end{aligned} \quad (\text{C5})$$

where

$$\kappa(\mathbf{v}') = \frac{1}{2} \left[G_+^h G_-^h + G_+ G_- \right] + F_+ F_-, \quad (\text{C6})$$

$$\lambda(\mathbf{v}') = F_+ F_-, \quad (\text{C7})$$

$$A_0 = - \lim_{\omega \rightarrow 0, \mathbf{q} \rightarrow 0} \left[G G^h + F F \right], \quad (\text{C8})$$

where, as before, the wave-function renormalization is set to unity. Keeping only the lowest order term in the expansion of the particle-particle interaction in Eq. (C3), one finds $1 - V_{\text{pp}}^0 A_0 = 0$, *i.e.*, the first two terms in that equation mutually cancel. (Note the different sign convention for V_{pp}^0 in the main body of the paper.)

We proceed now to solve these equations for the vertices in some cases of interest. For that purpose define the following integrals:

$$\alpha = \int \frac{d\Omega'}{4\pi} V_{\text{ph}}^{D/S}(\mathbf{v}\mathbf{v}') \lambda(\mathbf{v}'), \quad (\text{C9})$$

$$\eta = \int \frac{d\Omega'}{4\pi} V_{\text{ph}}^{D/S}(\mathbf{v}\mathbf{v}') \kappa(\mathbf{v}'), \quad (\text{C10})$$

$$\gamma = \int \frac{d\Omega'}{4\pi} V_{\text{ph}}^{D/S}(\mathbf{v}\mathbf{v}') \cos^2 \theta \lambda(\mathbf{v}'), \quad (\text{C11})$$

$$\beta = \int \frac{d\Omega'}{4\pi} V_{\text{ph}}^{D/S}(\mathbf{v}\mathbf{v}') \cos^2 \theta \kappa(\mathbf{v}'), \quad (\text{C12})$$

$$\psi = \int \frac{d\Omega'}{4\pi} V_{\text{ph}}^{D/S}(\mathbf{v}\mathbf{v}') \cos \theta \lambda(\mathbf{v}'), \quad (\text{C13})$$

$$\phi = \int \frac{d\Omega'}{4\pi} V_{\text{ph}}^{D/S}(\mathbf{v}\mathbf{v}') \cos^{-1} \theta \lambda(\mathbf{v}'). \quad (\text{C14})$$

In the following, we keep (as in the main body of this paper) the leading order Landau parameter in the particle-hole interaction amplitude, *i.e.*, $V_{\text{ph}}^{D/S}(\mathbf{v}\mathbf{v}') = v_{\text{ph}}$. Because κ and λ are even functions of $\cos \theta$, in this approximation the functions ϕ and ψ vanish. Following Leggett [28], we will use below the abbreviations

$$s = \frac{\omega}{qV_F} \quad u = \frac{qV_F}{\Delta}. \quad (\text{C15})$$

The longitudinal component in the vector channel, is obtained when $\xi^+ = 1$ and $\xi^- = 0$. Equations (C3) to (C5) are then written as

$$\begin{pmatrix} s^2 \alpha - \gamma & 2u\psi & -2su\alpha \\ v_{\text{ph}} u \psi & 1 - v_{\text{ph}} \eta & v_{\text{ph}} s \phi \\ -v_{\text{ph}} su \alpha & v_{\text{ph}} s \phi & 1 - v_{\text{ph}} (\eta - 2\alpha) \end{pmatrix} \begin{pmatrix} \tilde{\tau} \\ \tau^- \\ \tau^+ \end{pmatrix} = \begin{pmatrix} 0 \\ 0 \\ 1 \end{pmatrix},$$

As stated above $\phi = \psi = 0$ at leading order in the particle-hole interaction. The solution of this matrix equation is given by

$$\tilde{\tau} = \frac{2\Delta}{\omega} \frac{s^2 \alpha}{(s^2 \alpha - \gamma) [1 - v_{\text{ph}} Q_L]}, \quad (\text{C16})$$

$$\tau^+ = \frac{1}{1 - v_{\text{ph}} Q_L}, \quad (\text{C17})$$

and $\tau^- = 0$, where

$$Q_L \equiv \eta + \frac{2\alpha\gamma}{(s^2 \alpha - \gamma)}, \quad (\text{C18})$$

in agreement with Eqs. (52), (53) and (54) of Ref. [35] taken in the case of $V_{\text{ph}}^1 = 0$.

The longitudinal projection of the vector current polarization tensor is given by the expression [cf. [28], Eq. (23a)]

$$\Pi_{V,L} = \int \frac{d\Omega'}{4\pi} \xi^+ \left[\frac{\omega}{\Delta} \lambda \tilde{\tau} + \frac{\omega}{qV_F} \lambda \tau^- + (\kappa - 2\lambda) \tau^+ \right], \quad (\text{C19})$$

which after the substitution of the vertices becomes

$$\Pi_{V,L} = \left[\eta + \frac{2\alpha\gamma}{(s^2 \alpha - \gamma)} \right] \frac{1}{1 - v_{\text{ph}} Q_L} = \frac{Q_L}{1 - v_{\text{ph}} Q_L}. \quad (\text{C20})$$

By matching this equation to our result given by Eq. (61) we find

$$Q_L = \mathcal{A}^+ - \frac{\mathcal{D}^+}{\mathcal{C}} \mathcal{B} = \frac{\mathcal{Q}^+}{\mathcal{C}}. \quad (\text{C21})$$

The latter equality is straightforward to prove by noting that Eqs. (C7) and (C6) can be written in terms of the thermal function (A29) as

$$\lambda = \frac{\nu}{2} \mathcal{G}(\mathbf{v}, \omega, \mathbf{q}), \quad (\text{C22})$$

$$\kappa = \nu \left\{ \frac{(\mathbf{q}\mathbf{v})^2}{\omega^2 - (\mathbf{q}\mathbf{v})^2} \left[\mathcal{G}(\mathbf{v}, \mathbf{q}\mathbf{v}, \mathbf{q}) - \mathcal{G}(\mathbf{v}, \omega, \mathbf{q}) \right] \right\}. \quad (\text{C23})$$

We conclude that our result for the longitudinal vector current response function agrees with those given in Refs. [28, 35]. In particular, we have verified that the limiting cases of (i) $v_{\text{ph}} = 0$, (ii) $\omega \ll \Delta$, $qv_F \ll \Delta$ for non-zero T , and (iii) same as in (ii), but for $T = 0$, we recover the results of Ref. [35] by using the matching condition (C21). However, the perturbative result for the imaginary part of the longitudinal vector current response function in Ref. [35] [second term in Eq. (82)] differs from our result, given by Eqs. (95) and (B5) by a factor of 1/8. (Note that the author Ref. [35] used a density of state which is by a factor of 2 larger than ours). We have verified that one recovers our result by starting from the exact expression (C18) for Q_L and expanding the functions α , η and γ in small s^{-1} . In Ref. [35] the exact expression is first approximated by $Q_L \simeq \eta + 2s^{-2}\gamma$ after which the expansions for η and γ are substituted. The first step is the source of the discrepancy; we have verified that if the expansions of the functions α , η and γ are directly substituted in the exact expression (C18) for Q_L , then one recovers our result, which is also in agreement with the one quoted earlier by the authors of Refs. [34, 36].

In the case of the current response the bare vertices are given by $\xi = \mathbf{v}_\perp$ and $\xi^h = -\mathbf{v}_\perp$, *i.e.*,

$$\xi^+ = 0, \quad \xi^- = \mathbf{v}_\perp \quad (\text{C24})$$

where \mathbf{v}_\perp denotes the transverse to the momentum transfer projection of the quasiparticle velocity. If the momentum transfer is along the z axis, then $\mathbf{v}_\perp = v_F(\sin\theta \cos\phi, \sin\theta \sin\phi, \cos\theta)$. Keeping only the leading order Landau parameter in the particle-hole channel one finds

$$\tilde{\tau}^{(i)} = 0, \quad \tau^{+(i)} = 0, \quad \tau^{-(i)} = \mathbf{v}_\perp^{(i)}. \quad (\text{C25})$$

The anomalous vertex vanishes identically (the contributions to the vertex in the direction of the momentum transfer are neglected here). After substituting the vertices into the expression for the transverse part of the polarization tensor (Eq. (37) in Ref. [35]) we find

$$\Pi_{V,T} = \frac{v_F}{2} \int_{\Omega} \tau^- \kappa (1 - \cos^2\theta) = \frac{v_F^2}{2} (\eta - \beta), \quad (\text{C26})$$

which coincides with Eq. (86) of Ref. [35] when $v_{\text{ph}}^1 = 0$. The transverse vector response function is given according to Eq. (62) above. After substituting the explicit expression for the loop function \mathcal{A}^- from Eq. (A25) we use the relation (C23) to recover Eq. (C26), *i.e.*, the transverse vector polarization tensors are the same in both approaches. However, the perturbative expansions of these transverse polarization tensors differ, by a factor $O(1)$, *c.f.* Eq. (88) in Ref. [35] and Eqs. (96) and (B5) above.

The longitudinal and transverse axial-vector current polarization tensors of Ref. [35] can be matched to our results as in the case of vector current response functions, therefore we do not repeat the arguments above.

-
- [1] G. Baym and C. Pethick, *Ann. Rev. Astron. Astrophys.* **17**, 415 (1979).
[2] C. J. Pethick and D. G. Ravenhall, *Ann. Rev. Nucl. Part. Sci.* **45**, 429 (1995).
[3] U. Lombardo and H. J. Schulze, *Lect. Notes Phys.* **578**, 30 (2001).
[4] D. J. Dean and M. Hjorth-Jensen, *Rev. Mod. Phys.* **75**, 607 (2003).
[5] A. Sedrakian and J. W. Clark, in *“Pairing in Fermionic Systems: Basic Concepts and Modern applications”*, World Scientific, Singapore, 2006, p. 135.
[6] M. Baldo, O. Elgarøy, L. Engvik, M. Hjorth-Jensen, H.-J. Schulze, *Phys. Rev. C* **58**, 1921 (1998).
[7] M. V. Zverev, J. W. Clark, V. A. Khodel, *Nucl. Phys. A* **720**, 20 (2003).
[8] V. A. Khodel, J. W. Clark, M. V. Zverev, *Phys. Rev. Lett.* **87**, 031103 (2001).
[9] T. Alm, G. Röpke, A. Sedrakian and F. Weber, *Nucl. Phys. A* **604**, 491 (1996).
[10] E. Olsson and C. J. Pethick, *Phys. Rev. C* **66**, 065803 (2002).
[11] E. Olsson, P. Haensel and C. J. Pethick, *Phys. Rev. C* **70**, 025804 (2004).
[12] G. I. Lykasov, E. Olsson and C. J. Pethick, *Phys. Rev. C* **72**, 025805 (2005).
[13] G. I. Lykasov, C. J. Pethick and A. Schwenk, *Phys. Rev. C* **78**, 045803 (2008).
[14] C. J. Pethick and A. Schwenk, *Phys. Rev. C* **80**, 055805 (2009).
[15] J. Margueron, N. V. Giai and J. Navarro, *Phys. Rev. C* **72**, 034311 (2005).
[16] P. Bozek, J. Margueron and H. Müther, *Annals Phys. (NY)* **318**, 245 (2005).
[17] J. W. Negele and H. Orland, *“Quantum Many Particle*

- Systems*," (Addison-Wesley, New York, 1988).
- [18] B. L. Friman and O. V. Maxwell, *Astrophys. J.* **232**, 541 (1979).
- [19] A. Sedrakian and A. E. L. Dieperink, *Phys. Rev. D* **62**, 083002 (2000).
- [20] C. Hanhart, D. R. Phillips and S. Reddy, *Phys. Lett. B* **499**, 9 (2001).
- [21] R. G. E. Timmermans, A. Y. Korchin, E. N. E. van Dalen and A. E. L. Dieperink, *Phys. Rev. C* **65**, 064007 (2002).
- [22] A. Sedrakian and J. Keller, *Phys. Rev. C* **81**, 045806 (2010).
- [23] A. A. Abrikosov, L. P. Gorkov, *Sov. Phys. JETP* **8**, 1090 (1959); *Sov. Phys. JETP* **9**, 220 (1959).
- [24] A. A. Abrikosov, L. P. Gorkov, and I. E. Dzyaloshinski, *Methods of quantum field theory in statistical physics*, (Dover, New York, 1975).
- [25] N. Bogolyubov, *Nuovo Cimento* **7**, 794 (1958).
- [26] P. W. Anderson, *Phys. Rev.* **110**, 827 (1958).
- [27] A. I. Larkin and A. B. Migdal, *Sov. Phys. JETP* **17**, 1146 (1963); A. B. Migdal, *Theory of Finite Fermi Systems and applications to Atomic Nuclei* (Interscience, London, 1967).
- [28] A. J. Leggett, *Phys. Rev.* **147**, 119 (1966).
- [29] A. Sedrakian, *Prog. Part. Nucl. Phys.* **58**, 168-246 (2007).
- [30] J. Kundu and S. Reddy, *Phys. Rev. C* **70**, 055803 (2004).
- [31] L. B. Leinson and A. Perez, *Phys. Lett. B* **638**, 114 (2006).
- [32] A. W. Steiner, S. Reddy, *Phys. Rev.* **C79**, 015802 (2009).
- [33] A. Sedrakian, H. Mütter, P. Schuck, *Phys. Rev.* **C76**, 055805 (2007).
- [34] E. E. Kolomeitsev, D. N. Voskresensky, *Phys. Rev.* **C77**, 065808 (2008).
- [35] L. B. Leinson, *Phys. Rev. C* **79**, 045502 (2009).
- [36] E. E. Kolomeitsev and D. N. Voskresensky, *Phys. Rev. C* **81**, 065801 (2010).
- [37] A. Sedrakian, *Phys. Rev. C* **86**, 025803 (2012).
- [38] C. J. Pethick, N. Chamel and S. Reddy, *Prog. Theor. Phys. Suppl.* **186**, 9 (2010).
- [39] V. Cirigliano, S. Reddy and R. Sharma, *Phys. Rev. C* **84**, 045809 (2011).
- [40] A. Sedrakian, *Astrophys. and Space Sci.* **236**, 267 (1996).
- [41] L. Di Gallo, M. Oertel and M. Urban, *Phys. Rev. C* **84**, 045801 (2011).
- [42] B. Carter, N. Chamel and P. Haensel, *Nucl. Phys. A* **759**, 441 (2005).
- [43] B. Carter and E. Chachoua, *Int. J. Mod. Phys. D* **15**, 1329 (2006).
- [44] B. Carter and L. Samuelsson, *Class. Quant. Grav.* **23**, 5367 (2006).
- [45] M. Baldo and C. Ducoin, *Phys. Rev. C* **79**, 035801 (2009).
- [46] M. Baldo and C. Ducoin, *Phys. Atom. Nucl.* **74**, 1508 (2011).
- [47] M. Baldo and C. Ducoin, *Phys. Rev. C* **84**, 035806 (2011).
- [48] E. Flowers, M. Ruderman, P. Sutherland, *Astrophys. J.* **205**, 541 (1976).
- [49] D. G. Yakovlev, A. D. Kaminker and K. P. Levenfish, *Astron. Astrophys.* **343**, 650 (1999).
- [50] A. D. Kaminker, P. Haensel, D. G. Yakovlev, *Astron. Astrophys.* **345**, L14-L16 (1999).
- [51] V. G. Vaks, V. M. Galitski, A. I. Larkin, *Sov. Phys. JETP* **14** 1177 (1962).
- [52] E. E. Kolomeitsev and D. N. Voskresensky, *Phys. Rev. C* **84**, 068801 (2011).
- [53] J. Keller, Ph. D. Thesis, Frankfurt am Main, 2013.
- [54] D. N. Voskresensky, A. V. Senatorov, *Yad. Fiz.* **45**, 411 (1987) [*Sov. J. Nucl. Phys.* **45**, 657 (1987)].
- [55] N. W. Ashcroft and N. D. Mermin, *Solid State Physics* (Saunders College, Philadelphia, 1976).